UNIVERSITY OF TARTU
Faculty of Science and Technology
Institute of Technology

Gleb Zenjov

Screening of genes vital for the epithelial homeostasis with *Scribble* in *Drosophila* imaginal wing disc morphogenesis

Bachelor's Thesis (12 ECTS)
Curriculum Science and Technology

Supervisor(s):
PhD, Osamu Shimmi
MSc, Hanna Antson

Tartu 2023

Screening of genes vital for the epithelial homeostasis with *Scribble* in *Drosophila* imaginal wing disc morphogenesis

Abstract:

The model of *Drosophila melanogaster* wing imaginal disc has been used to study which growth factors are needed for tissue growth and what are the components for tissue to stop growing when it has reached its proper size. The sack-like structure of the wing disc is composed of epithelial cells and one of the characteristics of such cells is apico-basal polarity (ABP).

ABP is a critical factor that coordinates epithelial tissue homeostasis. The disruption of ABP leads to a complete loss of polarity and subsequent neoplasia formation. Scribble (Scrib) is one of the vital proteins that is involved in epithelial polarity determination and maintenance. Recent studies have revealed that the formation of neoplasia derived from local loss of Scrib depends on the copy number of Scrib within the tissue, providing a hypothesis that loss of Scrib-derived neoplasia formation is affected by additional genes having synergy with Scribble. To address this question, a gene screening was performed. The understanding of the hypothetical mechanism of how intercellular alignment occurs and which factors and genes are involved in homeostasis with Scrib has yet to be established.

The importance of genes is determined by using deficiency fly lines with deletion in specific genomic regions and the following conditional knockdown of *scrib* initiated by RNAi mechanism. The screening of previously established candidates allowed to narrow down the genomic region and to test the involvement of one of the potential genes - *Neurexin-IV* (*Nrx-IV*). Taken together, this study indicates that the genetic approach is valid and powerful for further investigating molecular mechanisms behind neoplasia/tumor formation.

Keywords:

Drosophila; wing imaginal disc; deficiency line; ABP; Scribble; gene screening.

CERCS:

B350 Development biology, growth (animal), ontogeny, embryology

Äädikakärbse tiiva imaginaaldiski epiteeli homöeostaasi säilitamisel osalevate geenide sõeluuring koos *Scribble* geeniga

Lühikokkuvõte:

Äädikakärbse (*Drosophila melanogaster*) areneva tiiva imaginaaldiski mudel on sobilik ja laialt kasutatav kudede kasvu uurimiseks, andes olulist infot milliseid kasvufaktoreid ja teisi molekulaarseid komponente on vaja koe kasvu reguleerimisel. Kudede morfogeneesis on oluline, et kasvamine peatuks kui õiged mõõtmed on saavutatud. Areneva tiiva eellane - tiivadisk - koosneb apiko-basaalselt (AB) polariseeritud epiteelirakkudest. AB polarisatsioon (ABP) on kriitilise tähtsusega epiteelikoe homöostaasi säilitamisel. Häired ABP-s võivad põhjustada rakkude polarisatsiooni täieliku kadumise, mis omakorda viib neoplaasia moodustumiseni. Üks oluline ABP-i moodustumise ja säilimise eest vastutavaid komponente on valk Scribble. Hiljutised uuringud on näidanud, et neoplaasia moodustumine on seotud Scribble funktsiooni lokaalsest kadumisest ning see on oluliselt sõltuv Scribble koopia arvust uuritavas koes. Sellest lähtuvalt püstitati hüpotees, et Scribble funktsiooni kadumisega seotud neoplaasia moodustumine on mõjutatud geenide poolt, millel on sünergia Scribble`ga. Teadmised selle kohta kuidas toimub rakkudevaheline koordineeritud regulatsioon epiteelkoe homöostaasi säilitamisel ja millised geenid/faktorid selles rolli mängivad koostöös Scribble valguga on puudulikud. Täitmaks seda lünka ja kontrollimaks hüpoteesi seati eesmärgiks läbi viia geneetiline sõeluuring koos *scribble* geeniga. Selleks kasutati uuritavate geenide puudulike kärbseliine, kus esines deletsioon spetsiifilistes genoomsetes piirkondades ning lisaks RNAi mehhanismiga *scribble* funktsiooni allasurumine. Kindlaks tehtud potentsiaalsete geenikandidaatide (faktorid, mis võiksid osaleda koos Scribble`ga epiteelkoe homöostaasi säilitamisel) sekundaarne sõeluuring võimaldas kitsendada genoomset piirkonda ja testida ühe uuritava geeni - *Neurexin-IV* (*Nrx-IV*) - sünergiat Scribble-ga. Kokkuvõttes näitasid antud bakalaurusetöös saadud tulemused, et selline geneetilise sõeluuringu lähenemine püstitatud küsimusele on suure potentsiaaliga meetod heitmaks valgust kantserogeneesi ja neoplaasia moodustumise tekkemehhanismidele.

Märksõnad:

Äädikakärbes, *Drosophila melanogaster*, tiiva imaginaaldisk, defitsiitne liin, apiko-basaalne polaarsus, Scribble, geeni sõeluuring

CERCS:

B350 Arengubioloogia, loomade kasv, ontogenees, embrüoloogia

TABLE OF CONTENTS

TERMS, ABBREVIATIONS AND NOTATIONS

A-P - anterior-posterior axis

ABP - apico-basal polarity

AJs - adherens junctions

aPKC - atypical protein kinase C

Baz - Bazooka

BMP - bone morphogenetic protein

Bou - Boudin

Crb - Crumbs

CyO - Curly-O

D - days (e.g. 3D - 3 days)

D-V - dorsal-ventral axis

DAPI - 4′,6-diamidino-2-phenylindole

Df - deficiency line

Dlg - Discs-large

Dpp - Decapentaplegic

dsRNA - double-stranded RNA

ECM - extracellular matrix

EMT - epithelial-mesenchymal transition

En - Engrailed

Ex - Expanded

FA - formaldehyde

Gal4 - galactose-responsive transcriptional activator in UAS/Gal4 system

$Gal80^{ts}$ - galactose-responsive temperature sensitive repressor of Gal4

GFP - green fluorescent protein

Hh - Hedgehog

HOOK - Dlg protein domain

Hu - Humeral

IgG - Immunoglobulin G

Inxs - innexins

KD - knock-down

Lgl - Lethal giant larvae

LOF - loss-of-function

LRR - leucine-rich repeat

LSR - lipolysis-stimulated lipoprotein receptor

Ly6 - Leukocyte antigen 6

MAGUK - membrane-associated guanylate kinase

Nrg - Neuroglian

Nrx-IV - *Neurexin IV*

Par - partitioning-defective complex

Patj - PALS1-associated homologue

PBS - phosphate-buffered saline

PBT - buffer used for imaging

Pos+ - positive-positive control

Pos - positive control

ptc - patched

PDZ - post synaptic density protein (PSD95), *Drosophila* disc large tumor suppressor (DlgA), and zonula occludens-1 protein (zo-1)

RISC - RNA-induced silencing complex

RNAi - RNA interference

RT - room temperature

SAR - subapical region

Scrib - *Scribble*

Sdt - Stardust

Sinu - Sinuous

siRNA - small interfering RNA

SJs - septate junctions

Tb - Tubby

TJs - tight junctions

TrJs - tricellular junctions

UAS - upstream activating sequence

Wg - Wingless

WT - wild type

Wts - Warts

YAP - Yes-associated protein

Yki - Yorkie

INTRODUCTION

Apico-basal polarity (ABP), being the specific characteristic of epithelial cells, is an important distinctive attribute that determines the precise locations of cellular composition. The correct alignment of those components is important for correct tissue organization, cell differentiation, and organ formation (Riga et al., 2020). Therefore, whenever one of the ABP-determining complexes gets disrupted, cells tend to lose the polarity that eventually leads to tumorigenesis (Enomoto & Igaki., 2011).

Basolaterally oriented Scribble (Scrib) complex consists of 3 proteins: Discs-large (Dlg), Lethal giant larvae (Lgl), and Scrib (Su et al., 2012). Scrib is a scaffold protein that is involved in coordination and preservation of the basal polarity of epithelial cells. Moreover, Scrib was recognized as a tumor suppressor, being one of the regulatory components of the Hippo signaling pathway, which when disrupted, often leads to tumours (Enomoto & Igaki., 2011; Huang et al., 2022).

The research in the thesis used the wing discs of *Drosophila melanogaster* as a model. Due to the very rapid development and relatively short life span, fruit flies have become a convencional organism to study various processes, including differentiation, development, metabolism, signaling pathways, effects of diseases and cancer, and much more (Bellen et al., 2010). The robust *Drosophila* toolkit has been developing since fruit flies were first used more than a hundred years ago and now includes thousands of tools and resources that allow the manipulation of the genome, the study of gene function, and the investigation of diverse biological processes (Roote, 2023). One of such toolkits is deficiency lines (Dfs) - the fly lines that lack one copy of some specific genomic region that allows the observation of the effects of gene deficiency on the organism (Roote, 2023).

Previous research has shown that the conditional knock-down of Scrib within the *patched* (*ptc*) region of the wing disc cells affected the surrounding cells and led to severe neoplasia, implying the significance of cellular communication via junctions in the process of cancer formation and spread (Huang et al., 2023). A subsequent screening of the left arm of the third chromosome was performed to pinpoint the genes that are involved in tissue homeostasis through intercellular alignment together with Scrib (Fischbach, 2022).

This thesis aims to perform a finer screening of one of the previously identified genomic regions, containing the genes involved in the ABP homeostasis with Scrib and to continue the screening of the right arm of the third chromosome.

1. LITERATURE REVIEW

1.1 Overview of fruit fly *Drosophila melanogaster* as a model

Drosophila melanogaster, also referred to as fruit fly, is a multicellular eukaryotic organism that has been used as a model organism for over a century. *D. melanogaster* (hereinafter referred to as *Drosophila*) has enabled scientists to study genetics, development in both physiological and pathological conditions, and more (Letsou & Bohmann, 2005).

One of the main advantages of using fruit flies as a model is their rapid life cycle. The embryogenesis of *Drosophila* takes about 10-14 days depending on the temperature of the environment (Figure 1) (Ong et al., 2015; Wangler & Bellen, 2017). The optimal temperature of 25 degrees allows the flies to develop in around 10 days whereas lower temperatures lead to longer developmental time of about 14 days. The life cycle consists of 4 different and distinct stages: embryonic and postembryonic (larval, pupal, and adult) stages. After the eggs are fertilized, the embryonic development into first instar larvae takes place within the first 24 hours. The larval stage lasts around 4.5-5 days and consists of 3 main phases: first, second, and third instar larval phases, during which the larvae enlarge, feed, and obtain all the required nutrients and energy for further growth and development (Ahmad et al., 2015). In the end of the third instar phase, larvae stop eating and form a puparium thereby entering the pupal stage. The pupal stage lasts around 3.5-4.5 days, during which complete metamorphosis occurs and the cells undergo final differentiation (Zeng et al., 2013). During the final, adult stage, after flies have hatched from the pupal case, they live around 2-3 months (Sun et al., 2013).

In the year 2000, the whole genome sequencing of *Drosophila* was conducted (Adams et al., 2000). This has led to the understanding that around 60% of known human genes and up to 75% of known human disease-associated genes have homologs in fruit flies (Fortini et al. 2000; Mirzoyan et al., 2019). This has given the opportunity to study not only human disease-related fields, such as Parkinson's, Alzheimer's, and cancer, but also viral interactions, drug discovery and responses, signaling pathways, and much more (Lessing & Bonini, 2009; Bellen et al., 2010; Apidianakis & Rahme, 2011; De Leemput & Han, 2021; Deolankar et al., 2022; Van Nainu et al., 2023).

The genome of *Drosophila* is packed into 4 pairs of chromosomes. The first is the pair of sex chromosomes (female XX, male XY), then two large pairs of chromosomes (the second and third chromosomes), and lastly the fourth chromosome. The fourth chromosome is very small compared to the other three, which is the reason why it is not as rigorously studied, as it

possesses lower gene density and is less likely to be associated with important genetic processes (Ashburner et al., 1999).

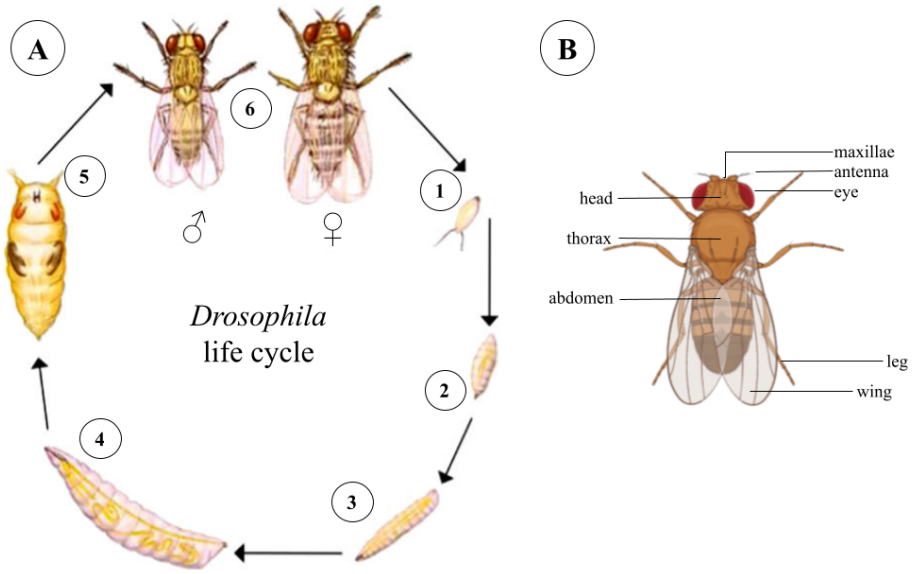

Figure 1. Life cycle of *Drosophila melanogaster*. A) (1-6) 6 main stages of *Drosophila* life cycle: embryonic stage (from fertilized egg cell to hatching larva) (1), postembryonic stages: larval stage (first (2), second (3), and third instar (4)), pupal stage (5), and adult stage (6). B) Structural units of *Drosophila*: 3 body parts - head, thorax and abdomen; 6 legs and 2 wings; the head has two conspicuous red eyes (wild-type (WT) files), a pair of antennae, and maxillae. Figure was modified from Wangler & Bellen, 2017 and created with https://biorender.com.

1.2 Fly genetics and molecular tools

1.2.1 Balancer chromosomes

Balancer chromosomes play an explicit role in fly genetics. Balancers enable the maintenance of clear genotypic identification based on the phenotype, as they possess markers that provide specific phenotypic changes in the fly that can be observed without any genomic analysis (Miller et al., 2019).

The introduction of a desired recessive mutation in *Drosophila* genome is not stable due to genetic drift. With a high probability it will eliminate the mutation in a small population of flies, even if it is advantageous. As *Drosophila* is a diploid organism, crossing over remains a crucial part of gametogenesis. The recombination of mutated alleles, either homozygous or heterozygous, would eventually lead to the loss of mutation, and the instrumentality of

balancer chromosomes serves to prevent such an outcome (Bloomington *Drosophila* Stock Centre (https://bdsc.indiana.edu/)). Balancers are genetically modified chromosomes possessing multiple nested inversions that prevent homologous recombination during meiosis by virtue of "incomplementarity" of homologous chromosomes (Miller et al., 2019). Therefore obtaining one copy of a mutated chromosome from one parent and the second copy of a balancer chromosome from another parent would create a heterozygous progeny. Two more genotypic outcomes are possible: a homozygous fly with two copies of mutant chromosomes, and homozygous fly with two copies of balancer chromosome, which is lethal for the flies (Hales et al., 2015).

As it is still important to differentiate between homozygous and heterozygous progenies, the balancer chromosome must have a dominant marker, causing a perceptible phenotype. Such markers bring up the ability to distinguish between the flies with and without a desired mutation. Selecting and self-crossing the progeny with a remarkable phenotypic appearance is essential for obtaining a stable fly stock (Hales et al., 2015).

There are dozens of classical balancers for all four chromosomes. The most used on the first chromosome are different variations of Fm7 (Fm7a, Fm7c, Fm7d, *etc.*), on the second chromosome Cyo, and on the third TM6B (Table 1). The ability to combine different markers has led to the creation of thousands of fly lines that are used for *Drosophila* research (Roote, 2023; Bloomington *Drosophila* Stock Center).

Table 1. Examples of classical dominant and recessive markers. *Drosophila* markers result in phenotypic changes: body colour and shape, eye colour and shape, wing size and structure, and bristle length and structure. The recognition, whether the marker is dominant or recessive, can be done by the first letter (capital letter - dominant; small letter - recessive). Collected from Roote (2023), Bloomington Stock Centre (https://bdsc.indiana.edu/), and FlyBase (https://flybase.org/).

Marker abbreviation and name	**Phenotype**
Cy (Curly)	Curly wings
w+ (mini white)	Yellow eyes
w (white)	White eye colour
Tb (Tubby)	Flattened body during pupal stage
Sb (Stubble)	Short abdominal and blunt bristles
cu (cutoid/curled)	Smooth abdomen
y+ (yellow)	Yellow body colour
e (ebony)	Dark body colour
Dr (Drop)	Small, drop-shaped eyes
Hu (Humeral)	Thicker thorax bristles

Curly-O or CyO is a second chromosome balancer, containing a curly (Cy) marker which twists the tips of fly wings, making them curled (Figure 2A). CyO balancer allows the recognition of flies carrying a mutant copy of a chromosome in the adult stage (Sun et al., 2012). Tm6B, in turn, has Tubby (Tb) and Humeral (Hu) dominant markers, which makes it possible to identify flies carrying the balancer not only in the adult stage, but also in larval and pupal stages. Larvae and pupae containing Tb marker look more compressed in comparison to the WT larvae and pupa (Figure 2B), whereas the adult flies do not seem to differ in body size and shape. The phenotype, indicating the presence of Hu in adult flies are the bristles on the dorsal thorax: compared to the WT, bristles are shorter, thicker, and their number is higher (Figure 2C) (Coutiño et al. 2021; Roote, 2023).

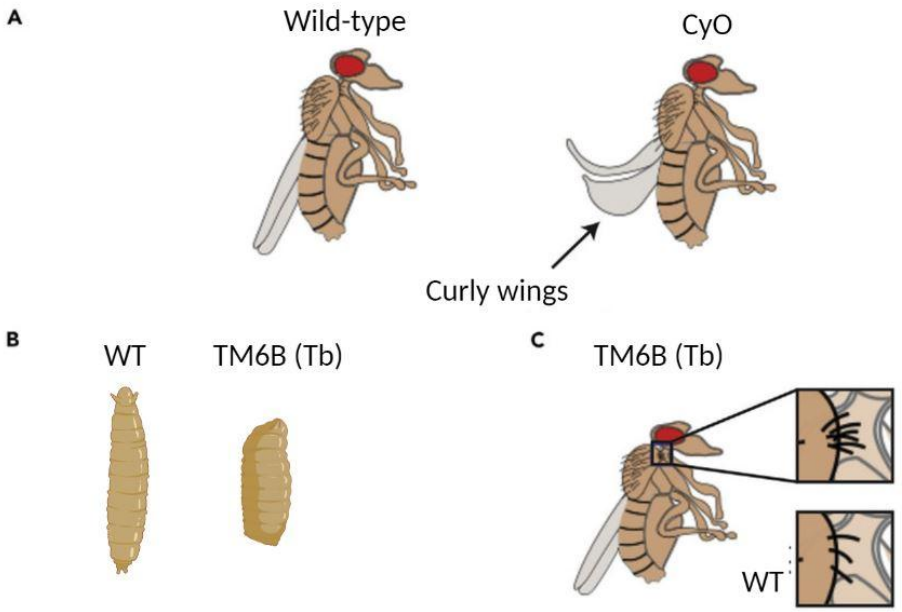

Figure 2. Phenotypic properties of CyO and TM6B/Tb balancers. (A) Phenotype comparison of a wild-type (WT) fly with a CyO-balanced fly. The wings of the CyO fly are curly, unlike the straight ones of the WT fly. (B) Comparison of a WT third instar larva (left) and larva with Tm6B balancer, containing Tb (Tubby) (right). The size and thickness of larva are the factors for Tb identification. The same applies for the pupal stage, as the size and thickness do not change. (C) Representation of Hu phenotype in adult flies (up) compared to WT (down). The Hu-balanced flies have a larger number of thorax bristles (compared to WT), which are thicker and smaller. Figure taken from Canales Coutiño et al., 2021 and modified with https://biorender.com.

1.2.2 RNA interference (RNAi)

RNA interference or RNAi is a cellular mechanism of gene silencing, which interacts with messenger RNAs (mRNAs) and not genes themselves (Figure 3) (Friedman & Perrimon, 2004). Its basis relies on the recognition of double-stranded RNAs (dsRNAs), appearance of which is associated with viral interactions and transcription of repetitive regions and transposable elements (Choudhary et al., 2007). The recognition leads to the binding of the RNase III enzyme (Dicer) to dsRNA and its cleavage into 20-25 nucleotide long sequences, which get unwounded and used as the template in RNA-induced silencing complex (RISC) to identify, cleave, and eventually degrade a complementary mRNA sequence. The mRNA molecule can no longer be translated, resulting in absence of the required protein (Fire et al., 1991; Fire et al., 1998). The discovery of the RNAi-based system in nematode *Caenorhabditis elegans* has led to the creation of a widely used technique for gene

knockdown (KD) and loss-of-function (LOF) studies in *Drosophila* both *in vitro* and *in vivo* (Fire et al., 1998).

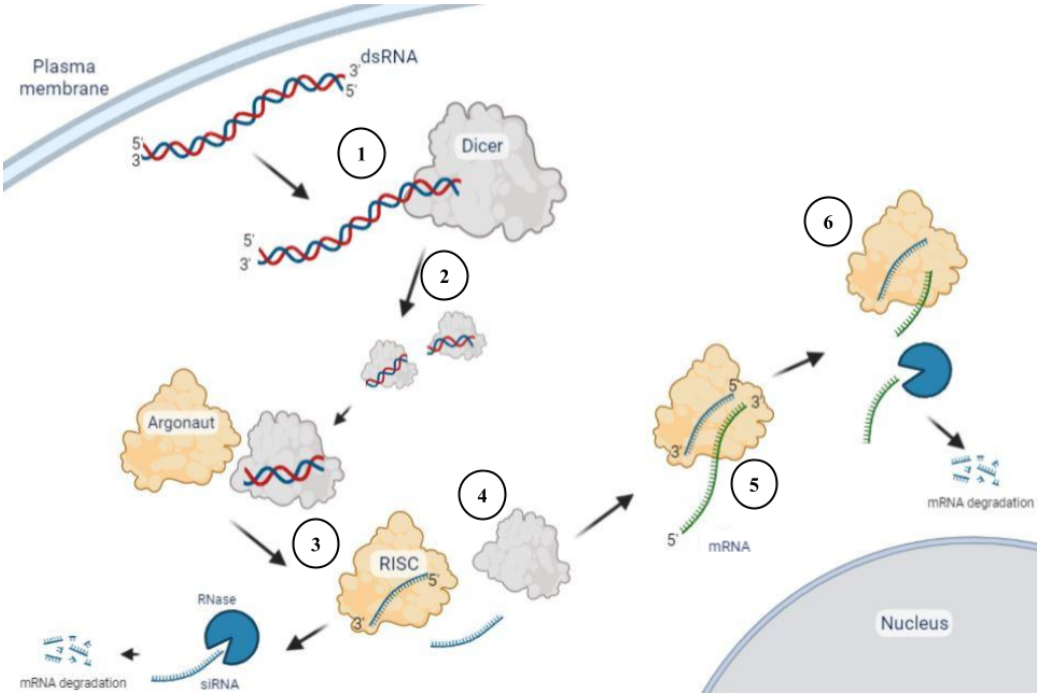

Figure 3. The mechanism of RNA interference. The double-stranded RNA (dsRNA) is recognized by Dicer enzymes which bind (1) and cleave (2) it into smaller units. Argonaut protein then binds to the dsRNA/Dicer complex (3) resulting in the yield of a RISC complex, a single-stranded molecule of small interfering RNA (siRNA) that eventually gets degraded, and a free Dicer (4). The RISC complex containing a 3'-5' siRNA molecule recognizes the mRNA with a complementary sequence (5), binds and catalyzes cleavage of messenger RNA (mRNA) (6) with its further degradation. The mechanism is used for gene down regulation, as it prevents the translation of cleaved mRNAs. Figure created with https://biorender.com.

1.2.3 UAS/GAL4/GAL80^{ts} system

The UAS/Gal4 gene regulation system was first introduced in flies 30 years ago (Brand & Perrimon, 1993). Since then, thousands of fruit fly lines possessing this system have been generated to get the insights into *Drosophila* development. Until this day, it is the most used method in *Drosophila* for regulating the expression of genes of interest in specific tissues (Barwell et al., 2017).

The UAS/Gal4 system consists of two main components: the Gal4 transcription factor, which binds to the upstream activation sequence (UAS), and the UAS-containing transgene, which is activated by Gal4. By placing the Gal4 transcription factor under the control of a tissue-specific promoter and using a UAS-containing transgene to express the gene of interest,

it is possible to direct the expression of the gene of interest in a specific tissue (Osterwalder et al., 2001).

The UAS/Gal4 method does not allow for temporal control of transgene expression, as the majority of the Gal4 promoters and enhancers are active in multiple developmental stages (Barwell et al., 2017). The introduction of temperature sensitive $Gal80^{ts}$ assists to overcome this problem, making it possible to create conditional KD conditions (Figure 4). $Gal80^{ts}$ acts as a Gal4 repressor under specific temperature conditions. At 18°C $Gal80^{ts}$ is bound to Gal4 and restricts the UAS/Gal4 activation and transcription of the gene of interest does not occur (Figure 4.1). At 29°C $Gal80^{ts}$ disassociates from Gal4, allowing Gal4 to induce the gene activation (Figure 4.2). By using the UAS/Gal4/$Gal80^{ts}$ system, it is possible to control and regulate gene expression in a spatio-temporal manner (Barwell et al., 2017).

To observe the resulting change of phenotype, a specific reporter must be introduced to be able to identify the precise localization of the protein of interest, as neither Gal4 nor $Gal80^{ts}$ are visible by themselves. The most commonly used reporter gene is Green Fluorescent Protein (GFP) that is being expressed downstream of UAS (Lam et al., 2022). However, other reporter proteins such as Red Fluorescent Protein (RFP) and channelrhodopsins can be used (Inagaki et al., 2014; He et al., 2019).

In addition to the UAS/Gal4 system, several other cognate systems with analogous mechanisms can be applied: LexA/LexAop, QF/QUAS, and rtTA/TetO (Venken et al., 2011).

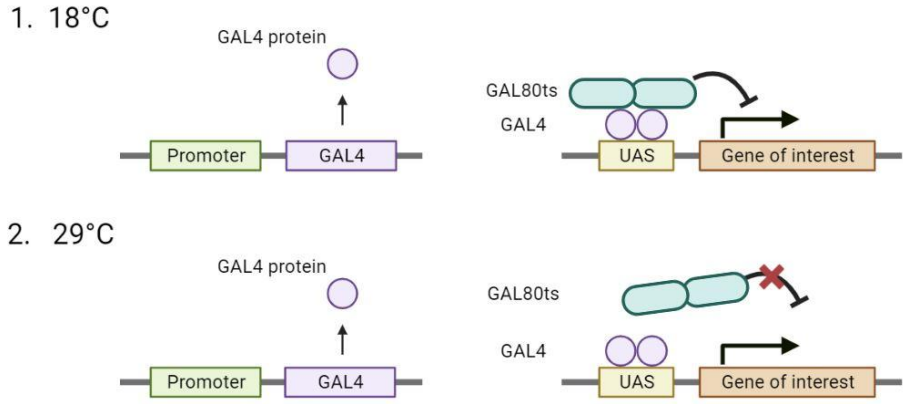

Figure 4. UAS/Gal4/Gal80^{ts} system. Gal4, being a gene expression activator, produces an eponymous protein, binding to regulatory sequence UAS, which allows the expression of the upcoming downstream gene. Gal80^{ts} is a temperature-sensitive protein that is capable of binding to Gal4 and restricting the transcription of the downstream gene. (1) At 18°C Gal80^{ts} acts as a repressor to Gal4, and the gene of interest is not expressed. (2) At 29°C Gal80^{ts} becomes inactivated and disassociates from Gal4, which recovers its activator role and the gene of interest is expressed. UAS/Gal4/Gal80^{ts} is an efficient toolkit that allows to regulate levels of expression of required genes by virtue of temperature differences. Figure created with https://biorender.com.

1.3 Epithelial cells

Epithelial cells are one of the major types of cells located in most organs, cavities, tubes, and body surfaces. These types of cells have a range of functions, the most significant being a protective barrier, uptaking and releasing substances, and facilitating the transportation of molecules within the cells. Nevertheless, specific functions of epithelial cells highly depend on their location (Tadeu & Horsley, 2014).

In general, being a "protective barrier" indicates that the epithelium tends to have vast amounts of bacterial and viral interactions, meaning they must possess strong immune recognition and response systems. Moreover, there are many types of cancers associated particularly with epithelial cells. Their abundance in various tissues, easy extraction techniques, and the ability to grow in cell culture makes them a useful model system for research (Duell et al., 2011; Holly et al., 2013).

1.3.1 Apical-Basal Polarity (ABP)

Homeostasis of cellular polarity is one crucial factor in epithelium formation and development. Apico-basal polarity (ABP) is a cell polarity characteristic of epithelial cells. It is sustained by the designated localizations of signaling molecules and protein complexes. Three main complexes responsible for establishing and maintaining ABP are Partitioning-defective (Par), Crumbs (Crb), and Scribble (Scrib) complexes (Figure 5). Par and Crb complexes are located at the apical, whereas Scrib complex is located at the basolateral compartment. In addition to establishing and maintaining ABP, these complexes are also needed for proper junctional alignments between the cells and organization of proper cytoskeletal arrangements within the epithelia (Enomoto & Igaki, 2011; Su et al., 2012).

Crb is composed of an integral membrane protein Crb, Stardust (Sdt), encoding membrane-associated guanylate kinase (MAGUK) (PALS1 in vertebrates), and PALS1-associated homologue (Patj) that is involved in tight junction (TJ) formation. The apical Par complex contains atypical protein kinase C (aPKC), which is actively involved in Lethal Giant Larvae (Lgl) phosphorylation, Bazooka (Baz) that interacts with adherens junctions (AJs), and Par6, which is related to controlling cell proliferation. The Scribble complex is aligned basolaterally and consists of Dlg that is involved in septate junctions (SJs) formation and signal transduction, Lgl that is responsible for asymmetric distribution of cellular macromolecules, and Scrib (discussed in section 1.3.2) (Moscat & Diaz-Meco, 2000; Nolan et al., 2008; Chen et al., 2010; Cao et al., 2015; Campanale et al., 2017; Rust & Wodarz, 2021; https://flybase.org).

The apical and basal regions of a cell have different responses to signaling molecules from the environment and neighboring cells, which allow cells to coordinate their molecular behaviour and properly respond to changes in the surroundings. ABP coordination is vital for establishing correct tissue architecture and determining cell fates during development (Riga et al., 2020). Disruption of any protein in one of the complexes related to cell polarity determination and regulation leads to the disarrangement of the complex. Additionally, the disruption of one complex will lead to the disruption of other two complexes and subsequently to the complete loss of ABP, ultimately proceeding with epithelial-mesenchymal transition (EMT) and malignant tumour genesis (Jung et al., 2019; Riga et al., 2020).

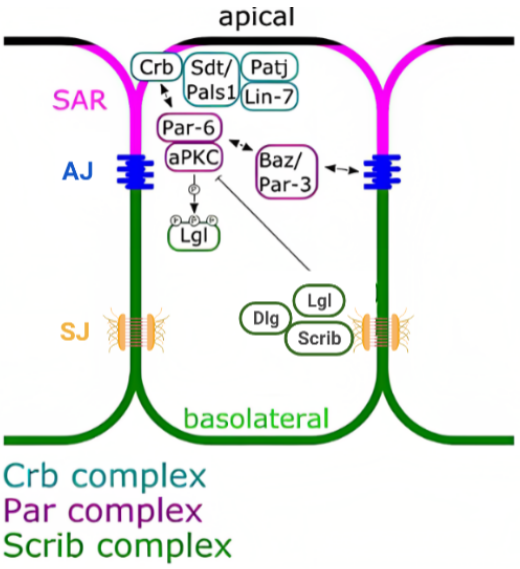

Figure 5. *Drosophila* ABP-determination complexes and their components in epithelial cells. Three crucial complexes determine ABP: Crb (blue), Par (pink), and Scrib (green). Crb and Par are located on the apical side of the cell and interact in SAR (subapical region). Scrib complex is located at the basolateral side of the cell and negatively regulates the kinase aPKC that phosphorylates Lgl. Arrows indicate interactions of different components of the complexes. AJs (blue) and SJs (yellow) are presented as examples of epithelial junctions. Figure adapted and modified from Rust & Wodarz, 2021.

1.3.1.1 Cell-cell adhesions (junctions)

Two major types of epithelial junctions in *Drosophila* are adherens junctions (AJs) and septate junctions (SJs), but others like gap junctions and tricellular junctions (TrJs) can also be found in *Drosophila* epithelial cells (Badouel & McNeill, 2009; Higashi & Miller, 2017). The functions of cellular junctions highly depend on their composition and they have different tasks. These include firstly the cell-to-cell attachments that create a barrier between the cells to prevent diffusion of unnecessary molecules. Secondly, the adhesion for structural unit formation or creation of the channel, by which intercellular transport of small molecules can be implemented, and thirdly the cell-to-ECM (extracellular matrix) attachments (Badouel & McNeill, 2009).

AJs are located at the lateral side of epithelial cells forming a belt-like structure. They provide mechanical stability to tissues by holding cells together and regulating cell behavior through cell signaling. AJs core components involve transmembrane cadherin-catenin components, such as DE-cadherin, Arm (β-catenin), α-Catenin, and p120-Catenin. The Crumbs complex is known to be located near AJs (see section 1.3.1) (Harris, 2012; Sen et al., 2012).

SJs, analogs of tight junctions (TJs) in vertebrates, serve the role of trans-epithelial barrier formation which is required for the restriction of unwanted molecule diffusion between the cells. Moreover, as SJs are located at the basolateral plasma membrane region, they are involved in establishing and maintaining ABP and mediating signal exchange between the cells (Rice et al., 2021).

Around 30 proteins are involved in the formation of SJs and can be categorized as core compositional proteins, SJ resident proteins, and accessory proteins. Core SJ proteins, such as Neurexin IV (Nrx-IV), Nrg, and Sinu are required for the composition and establishment of the junctions. They contain extracellular domains involved in protein-protein and protein-ECM interactions. Additionally, their interactions with actin filaments support linkage between SJs and cytoskeleton. SJ resident proteins Dlg, Scrib, and α-Catenin bind to fully developed SJs, but are not required for their maintenance and assembly. SJ accessory proteins, like Ly6, Bou, and others are required for the maintenance of the junctions, but are not involved in their composition (Müller, 2000; Rice et al., 2021; De et al., 2022; Huang et al., 2022; Huang et al., 2023).

Gap junctions represent aqueous pores that connect two adjacent cells and allow the exchange of ions and small molecules. Invertebrate gap junction multimeric channels are composed of innexins (Inxs), which create a 2-4 nm gap between two neighboring cell membranes, allowing a passive exchange of signaling molecules, small metabolites, and secondary messengers (Stebbings et al., 2002; Mese et al., 2007).

Additional types of intercellular junctions in *Drosophila* are tricellular junctions (TrJs). They have a role of barrier creation, as TJs and SJs, but are distinct by the fact that they appear when contact between three cells is required (Higashi & Miller, 2017). TrJs are composed of a variety of transmembrane and cytoplasmic proteins, including tricellulin protein, lipolysis-stimulated lipoprotein receptor (LSR), angulin family proteins, and MAGUK family proteins. The other components of tricellular junctions depend on the type of junctions that are formed, as the connections can be formed not only between SJs, but also AJs (Higashi & Miller, 2017).

1.3.2 Scribble

The Scribble (Scrib) complex is one of the three essential protein complexes needed for establishing and maintaining ABP. It is located at the basolateral apex of epithelial cells. The Scrib complex consists of three proteins: Discs-large (Dlg), Lethal giant larvae (Lgl), and Scrib. Together they are responsible for establishing and maintaining ABP and the

maintenance of SJs. Disruption of any of the three proteins within the complex will lead to the loss of ABP and the formation of neoplasia caused by uncontrolled cell proliferation. Dlg has been recognized as the homolog of MAGUK, containing two of its domains (PDZ2 and HOOK). They were identified in the subcellular localization of the plasma membrane, which strengthened the association of Dlg with SJs formation (Su et al., 2012). Lgl plays an important role in epithelial asymmetrical cell division of neuroblasts and contributes to the formation of actin-rich projections at the oocyte cortex and the posterior enrichment of Par1 (https://uniprot.org). The disruption or loss of Lgl during embryogenesis results in the death of *Drosophila* before entering the pupal stage (De Lorenzo et al., 1999).

Scribble, the third protein comprising the complex, is a cytoplasmic protein, consisting of 1751 amino acids. Scrib is primarily composed of multiple copies of two regulatory sequence types: leucine-rich repeats (LRR), which are enrolled in SJs protein localization and protein-ligand interactions, and PDZ domains that assist protein-protein interactions and Scrib stabilization (Figure 6.1) (Zeitler et al., 2004; Helft et al., 2011; Barreda et al., 2020; Gui et al., 2021).

The sequence analysis of the *scrib* locus revealed 7 alleles, 6 of which being sequences possessing nonsense mutations, forcing an appearance of premature stop codons, and the seventh WT gene ($scrib^{1\text{-}7}$) (Figure 6.1) (Zeitler et al., 2004). *Drosophila* imaginal wing disc screening showed the diversified intensity of ABP loss depending on the portion of the partially lost Scrib protein (Figure 6.2). The results showed more severe tissue neoplasia phenotype in imaginal discs that lacked larger amino acid sequences. Moreover, it was confirmed that the loss of one or more PDZ regions did not lead to the full destruction of ABP and thereby led to less severe tumour phenotype, whereas Scrib lacking portions of LRR regions and PDZ domains could not maintain the preservation of epithelium and acute tumorous structures were apparent. Thus when the LRR domain is intact, the epithelial monolayer is still able to develop (Zeitler et al., 2004). $scrib^{2}$, which results in nearly full loss of functional allele, was therefore considered to be a null allele causing the major disruption of ABP and is often used in the research of ABP mechanism (Zeitler et al., 2004).

Knockdown and sequential variants of Scrib that vary in length of their sequences were shown to disrupt the homeostasis of ABP, while the overexpression of *scrib* was subsequently shown to enhance the stability of ABP, thereby unravelling its property to be an epithelial tumour suppressor (Kapil et al., 2017; Gui et al., 2021).

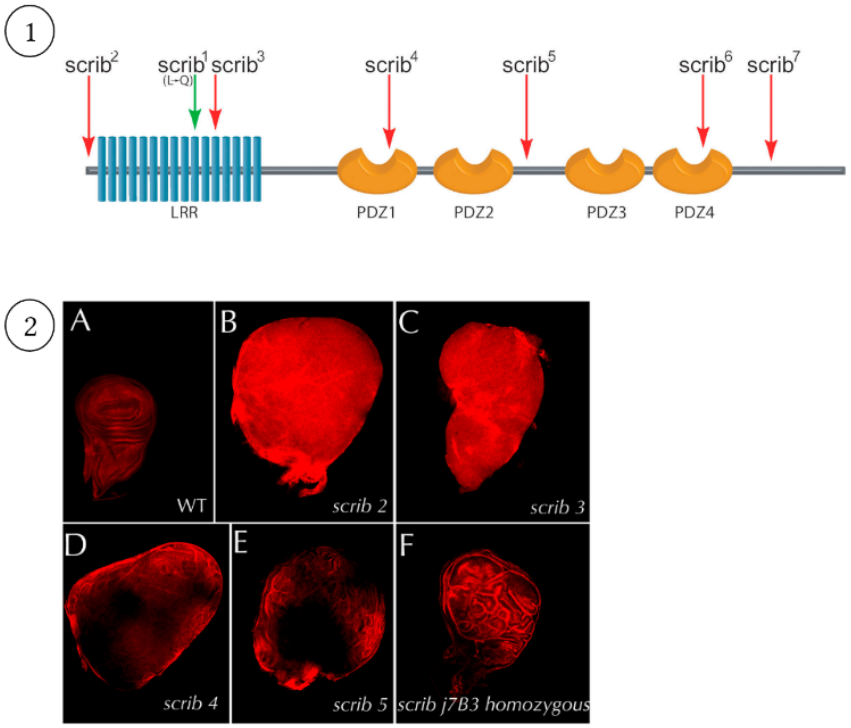

Figure 6. Scribble protein variants and their impact on imaginal wing disc phenotype. Scrib is one of the three proteins composing the Scrib complex, essential for ABP homeostasis. (1) Sequential composition of *scrib* gene. 7 alleles of the gene have been identified: $scrib^{7}$ being the wild type sequence and $scrib^{1\text{-}6}$- genes with occurrence of premature termination codons. Red arrows indicate the premature stop codons of *scrib* variants; green arrow indicates a missense mutation, occurring in $scrib^{1}$. (2) Images of *Drosophila* imaginal wing discs containing various Scribble alleles (A-F). Every *scrib* variant besides the wild type (A) shows the disc overgrowth and overproliferation of epithelial tissue caused by the loss of ABP (B- $scrib^{2}$, C- $scrib^{3}$, D- $scrib^{4}$, E- $scrib^{5}$, F- $scrib^{j7B3}$ (homozygous for mutated allele)). Figure adapted and modified from Zeitler et al., 2004.

Additionally, Scrib has been shown to play an important role in the regulation of the highly conserved Hippo signaling pathway that regulates cell growth, proliferation, and apoptosis (Figure 7) (Verghese et al., 2012). In *Drosophila*, the Hippo pathway regulates the transcriptional co-activator Yorkie (Yki), the homolog of mammalian Yes-associated protein (YAP). Specifically, Scrib has been shown to interact with the Hippo pathway kinase Warts (Wts) to promote its localization and activation. Moreover, Scribble also interacts and regulates the activity of the scaffolding protein Expanded (Ex) on the apical domain, where it interacts with and activates Wts. This in turn leads to the phosphorylation of Yki and the inhibition of Yki-dependant gene expression. The disruption of the Scrib complex results in Yki translocation into the nucleus where Yki-dependant genes responsible for proliferation

will lead to the overgrowth of tissues. Therefore, the reliance of Scribble to phosphorylate Yki and prevent its translocation into the nucleus is a critical aspect of its tumour suppressive role, and dysregulation of Scrib leads to compromised Hippo signaling pathway (Yu & Pan, 2018; Snigdha et al., 2019; Gui et al., 2021).

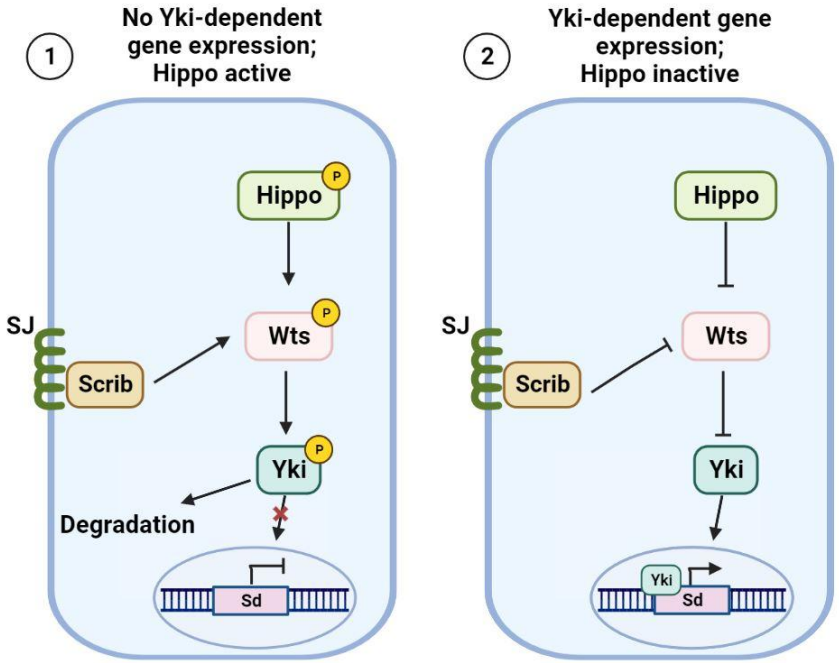

Figure 7. Hippo signaling pathway components associated with transcriptional coactivator Yki. (1) Active Hippo signaling pathway. In addition to Hippo, Scrib interaction leads to the phosphorylation of Warts kinase (Wts). This results in interactions between phosphorylated Wts and Yki, leading to the phosphorylation and subsequent degradation of Yki. As a result, Yki is unable to translocate into the nucleus and bind to Scalloped (Sd) and no Yki-dependent gene expression occurs. (2) Inactive Hippo signaling pathway. Disruption of the Scrib complex leads to compromised Hippo pathway. As a result, Wts is not phosphorylated and no Yki phosphorylation occurs. This allows unphosphorylated Yki to translocate into the nucleus and bind to Sd leading to the expression of Yki-dependent genes. Figure created with https://biorender.com.

Furthermore, it was identified that WT Scrib cells can influence neighbouring hypomorphic mutant Scrib cells and *vice versa*. It was shown that Scrib mutant cells that are surrounded by WT cells have their ABP non-autonomously restored, strongly suggesting the presence of a signaling compensational mechanism (Huang et al., 2022). The precise model and components involved in signal transduction between epithelial cells are yet to be established, but the current hypothesis suggests the existence of a feed-forward mechanism (Figure 8). It states that the loss of ABP due to absence of basolateral component Scrib leads to

hyperactivation of Yki, increasing the loss of ABP and intensifying neoplasia formation (Huang et al., 2022).

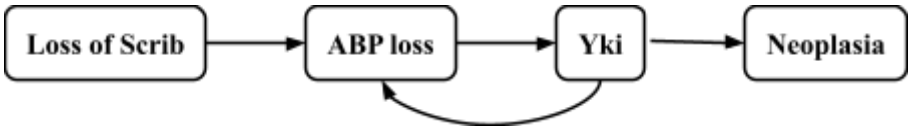

Figure 8. Hypothetical feed-forward mechanism of neoplasia formation. The current proposition suggests that loss of Scrib leads to loss of ABP. This leads to subsequent activation of Yki, which in turn exacerbates additional loss of APB and increases neoplasia formation. Created on the basis of Huang et al., 2023.

Current data presents strong evidence of involvement and interactions of junctional components, such as α-Catenin with Scrib. Additionally, the data obtained by our lab using *scrib* RNAi flies showed that conditional KD of Scrib (2 days) only affects α-Catenin, but not β-Cadherin and E-Cadherin, two important components of AJs. The long-term KD (3-4 days) significantly influenced other junctional components, which provides explicit evidence of gradual and progressive disruption of epithelial tissue (Huang et al., 2023).

1.4 Imaginal wing disc

Drosophila imaginal discs represent integral clusters of undifferentiated monolayers of progenitor cells during embryogenesis that invaginate into structural units in adult flies, such as eyes, legs, antennae, genitalia, and wings (Ostalé et al., 2018).

The wing imaginal discs have become a powerful tool for studying gene regulatory networks, signaling pathways, cell proliferation, patterning, and much more for several reasons. Primarily due to the high rates of cell division. Starting from the first instar larval stage, the primordial wing disc consists of around 30 cells and their number exceeds 35,000 by the end of the third instar stage. This indicates that the third instar larvae allow to create a very good model to study molecular mechanisms and pathways, and how tissue growth and patterning is controlled (Neto-Silva et al., 2009; Tripathi & Irvine, 2022).

Secondly, flies kept in laboratory conditions do not require wings for proper survival and reproduction, thus wing imaginal discs are good targets for genetic manipulations (Ostalé et al., 2018).

The morphogenesis of wing imaginal discs is a critical aspect, involving dynamic cellular behaviors such as cell migration, changes in cell shape, and cell-cell adhesion that is strictly regulated by various signaling pathways, including Notch, Wnt/Wingless (Wg), Bone morphogenetic protein/Decapentaplegic (BMP/Dpp), and Hedgehog (Hh) (Aegerter-Wilmsen et al., 2007; Hatori & Kornberg, 2020).

The third instar larval wing imaginal disc can be divided into three distinct areas: notum, hinge, and wing pouch region, latter of which the future wing blade invaginates from. The disc structure can also be divided with two axes: anterior-posterior (A-P), determined by En-Hh pathway, and dorsal-ventral (D-V), which is being regulated by Ap-Notch pathway (Figure 9). The joints of two regions create barriers, defined by cell-lineage restrictions, so the cells from different compartments cannot cross on to the other side. Cells located at the barriers can control the expression of transcriptional activators and repressors for the barrier sustainability and control of tissue differentiation (Diaz De La Loza & Thompson, 2017).

Each region of the wing disc will have a distinct combination of Hox genes that determine segmental identity, cell fates, and presage the final differentiated adult wing structure (Tripathi & Irvine, 2022).

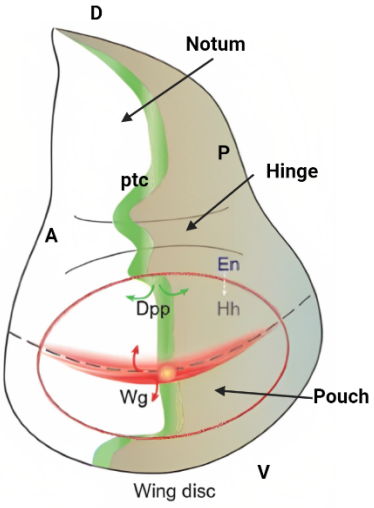

Figure 9. Structural areas of *Drosophila* wing imaginal disc. Epithelial cells of the wing disc can be categorized in distinct subregions, including the pouch (on ventral side (V)), hinge, and notum (on dorsal side (D)). The disc is split in half by the *patched* (*ptc*) region, controlled by Dpp and creating anterior (A) and posterior (P) sides. The cells in the pouch region are mainly controlled by Wg and Hh signaling pathways, while the hinge region prevails in a homeodomain transcription factor Engrailed (En). Figure adopted and modified from Beira & Paro, 2016.

1.5 Deficiency lines

Deficiency lines (Dfs) have been a part of *Drosophila* toolkit for several decades. The term "Df" is used to refer to the fly stock possessing a deficiency in their genome - the deletion of a specific DNA sequence, containing one copy of a functional gene, leaving the organism in a haploid state for that gene (Roote, 2023).

The basis of Dfs lies in the deletion of length-varying genomic regions across the whole fly genome, containing single or multiple genes that are not required in a diploid state for the organism to survive. This technique allows to define the effects of gene loss on multiple stages of the life cycle and understand their involvement in cellular and developmental processes (Wright et al., 2010). Introduction of systems that allow genetic manipulations depending on environmental conditions and genetic background, such as UAS/Gal4/Gal80^{ts}, GFP markers, and various gene RNAi's establish a possibility of gene conditional KD that enables the determination of the functions of genes located on a deleted region (Roote & Russell, 2012).

Such a method raises an issue of haploinsufficiency, when the deleted region contains genes vital for the development and survival of the organism, and their loss leads to a lethal outcome. To prevent this, essential DNA-containing sequences are being translocated to other chromosomal regions in order to keep the organism diploid for them (Roote, 2023).

Thousands of Dfs have been created for numerous research purposes and can be purchased from stock centers, such as Bloomington or Kyoto, where all the important information about them is available and connected with the FlyBase database.

2. THE AIMS OF THE THESIS

The ongoing projects in the host lab aim to identify genes that cooperate with Scrib in maintaining tissue homeostasis. Identification of such genes is crucial for understanding the molecular mechanisms underlying proper intercellular communication, cooperation, and epithelial morphogenesis.

Previous results established conditions of conditional *scrib* RNAi and dosage dependency of *scrib* in RNAi (Fischbach, 2022; Huang et al., 2022). Therefore, we hypothesize that Scrib has synergy with other genes related to the progression of neoplasia. For that we plan to conduct a whole third chromosome screening to narrow down the chromosomal regions and identify new candidate genes.

The establishment of a proper protocol is another important factor, as incorrect timing and temperature conditions can lead to false results.

Thus, the aims of the thesis are following:

- Conduct a finer screening of the left arm of the third chromosome Dfs that were previously confirmed to have ABP disruption and resulting in neoplasia phenotype.

- Perform a partial screening of the right arm of the third chromosome Dfs to detect the chromosomal regions containing potential candidate genes which have a synergy with Scrib and are involved in ABP establishment.

- Establish or contribute to the establishment of the screening protocol with updated conditions.

3. EXPERIMENTAL PART

3.1 MATERIALS AND METHODS

3.1.1 Fly lines

The study of wing imaginal discs has been facilitated by the availability of genetic tools and techniques, such as mutagenesis, transgenic technologies, and RNAi. Thousands of *Drosophila* lines have been created for these purposes and are available from stock centers, e.g. Bloomington *Drosophila* Stock Center (BDSC; https://bdsc.indiana.edu/index.html).
The ongoing project is based on Df screening, which was made possible by the deficiency toolkit obtained from the BDSC (https://bdsc.indiana.edu/stocks/df/dfkit-info.html).
The precise genotype must be determined, thus various fly flies were used (Table 2). Besides Dfs, fly lines for UAS/Gal4/Gal80^{ts} systems, controls and balancer chromosomes were utilized.

Table 2. Fly lines used in the thesis.

Line number in Bloomington	Genotype	Type, purpose
1990 [Df(3R)Tpl10]	Df(3R)Tpl10, Dp(3;3)Dfd[rv1], kni[ri-1] Dfd[rv1] p[p] Doa[10]/TM3, Sb[1]	Df, primary screening
4380	ru[1] hry[1] Nrx-IV[4304] st[1] ry[506] e[1]/TM6B, Tb[+]	*nrx-IV* mutant allele
6962 [Df(3R)ED2]	w[1118]; Df(3R)ED2, P{w[+mW.Scer\FRT.hs3]=3'.RS5+3.3'}kok o[ED2]/TM6C, cu[1] Sb[1]	Df, primary screening
7443 [Df(3R)BSC47]	Df(3R)BSC47, st[1] ca[1]/TM3, P{w[+m*]=Ubx-lacZ.w[+]}TM3, Sb[1]	Df, primary screening
7595 [Df(3L)Exel6116]	w[1118]; Df(3L)Exel6116, P{w[+mC]=XP-U}Exel6116/TM6B, Tb[1]	Df, secondary screening
7680 [Df(3R)Exel6201]	w[1118]; Df(3R)Exel6201, P{w[+mC]=XP-U}Exel6201/TM6B, Tb[1]	Df, primary screening
7682 [Df(3R)Exel6203]	w[1118]; Df(3R)Exel6203, P{w[+mC]=XP-U}Exel6203/TM6B, Tb[+]	Df, primary screening
7692 [Df(3R)Exel6214]	w[1118]; Df(3R)Exel6214, P{w[+mC]=XP-U}Exel6214/TM6B, Tb[1]	Df, primary screening

7737 [Df(3R)Exel6270]	w[1118]; Df(3R)Exel6270, P{w[+mC]=XP-U}Exel6270/TM6B, Tb[1]	Df, primary screening
7997 [Df(3R)Exel7378]	w[1118]; Df(3R)Exel7378/TM6B, Tb[1]	Df, primary screening
8029 [Df(3R)ED5577]	w[1118]; Df(3R)ED5577, P{w[+mW.Scer\FRT.hs3]=3'.RS5+3.3'}ED 5577/TM6C, cu[1] Sb[1]	Df, primary screening
8069 [Df(3R)ED4475]	w[1118]; Df(3L)ED4475, P{w[+mW.Scer\FRT.hs3]=3'.RS5+3.3'}ED 4475/TM6C, cu[1] Sb[1]	Df, main candidate line for secondary screening
8070 [Df(3R)ED4483]	w[1118]; Df(3L)ED4483, P{w[+mW.Scer\FRT.hs3]=3'.RS5+3.3'}ED 4483/TM6C, cu[1] Sb[1]	Df, secondary screening
8105 [Df(3R)ED6232]	w[1118]; Df(3R)ED6232, P{w[+mW.Scer\FRT.hs3]=3'.RS5+3.3'}ED 6232/TM6C, cu[1] Sb[1]	Df containing *scrib* locus, used for positive-positive control (Pos+)
9501 [Df(3R)BSC141]	w[1118]; Df(3R)BSC141/TM6B, Tb[+]	Df, primary screening
23232	w[*]; ry[506] Dr[1]/TM6B, P{Dfd-GMR-nvYFP}4, Sb[1] Tb[1] ca[1]	Dr/Tb balancer
24420 [Df(3L)BSC396]	w[1118]; Df(3L)BSC396/TM6C, Sb[1] cu[1]	Df, secondary screening
24962 [Df(3R)BSC458]	w[1118]; Df(3L)BSC458/TM6C, Sb[1] cu[1]	Df, secondary screening
26527 [Df(3R)BSC675]	w[1118]; Df(3L)BSC675, P+PBac{w[+mC]=XP3.WH3}BSC675/T M6C, Sb[1] cu[1]	Df, secondary screening
26528 [Df(3R)BSC676]	w[1118]; Df(3L)BSC676/TM6C, Sb[1] cu[1]	Df, secondary screening
26579 [Df(3R)BSC727]	w[1118]; Df(3L)BSC727/TM6C, Sb[1] cu[1]	Df, secondary screening
26828 [Df(3R)BSC730]	w[1118]; Df(3L)BSC730/TM6C, Sb[1] cu[1]	Df, secondary screening
29024 [Df(3L)BSC840]	w[1118]; Df(3L)BSC840, P+PBac{w[+mC]=XP3.RB5}BSC840/TM 6C, Sb[1] cu[1]	Df, secondary screening
32434	y[1] sc[*] v[1] sev[21]; P{y[+t7.7] v[+t1.8]=TRiP.HMS00419}attP2/TM3,	*nvr-IV* RNAi III

	Sb[1]	
39071	y[1] sc[*] v[1] sev[21]; P{y[+t7.7] v[+t1.8]=TRiP.HMS01991}attP40	*nrx-IV* RNAI II
N/A	+/+; ptc-Gal4, UAS-GFP, ex-LacZ/CyO; Scrib RNAi, Gal80^{ts}/Scrib RNAi, Gal80^{ts}	Host stock, used for Df crosses and as a positive control (Pos)
N/A	ex-LacZ, ptc-Gal4, UAS-GFP; scrib:GFP, GFP RNAi/Tm6	*scrib*^{2}
N/A	ptc-GAL4; TubP-Gal80^{ts}, UAS-Tub-mCherry	Used as a negative control for *nrx-IV* screening

3.1.2 Fly crosses

The main type of crosses used in the experiments were Dfs crossed with the *scrib* RNAi host stock (Figure 10). The host stock was generated specifically for the project by our lab (Huang et al. 2022). By using *patched* (*ptc*)-Gal4 driver, it is possible to knock-down *scrib* in a specific stripe region in the middle of the pouch region of the wing imaginal disc (Figure 9). The *scrib* RNAi host stock is crossed with the Df over the Tm6B balancer, which is needed for genotype identification of the required progeny during third instar larvae. The desired genotype on the third chromosome (Figure 10A) acquires the *scrib* RNAi-Gal80^{ts} for the conditional KD of *scrib* under the deficiency line of interest. The identification of the desired genotype on the third chromosome is possible due to the absence of Tb balancer (Figure 10A, C). The fluorescent stereo microscopy is then used to distinguish the correct genotype on the second chromosome by the GFP expression in the wing imaginal discs (Figure 10A, C) (see section 3.1.4.1). The progeny with Tb (Figure 10C, D) does not contain the deficient region and is excluded.

All Df stocks must be balanced over the Tm6B balancer for the proper experiment. Original fly lines obtained from the Bloomington Stock Center are often balanced by the other balancer chromosome (Table 2), thus they must be switched to be under the Tm6B balancer. Dfs are crossed with Dr/Tm6B Tb Sb flies and the progeny is examined based on the Tb and Sb phenotypes (Table 1) and collected for the self-crossing that generates desired Df stocks.

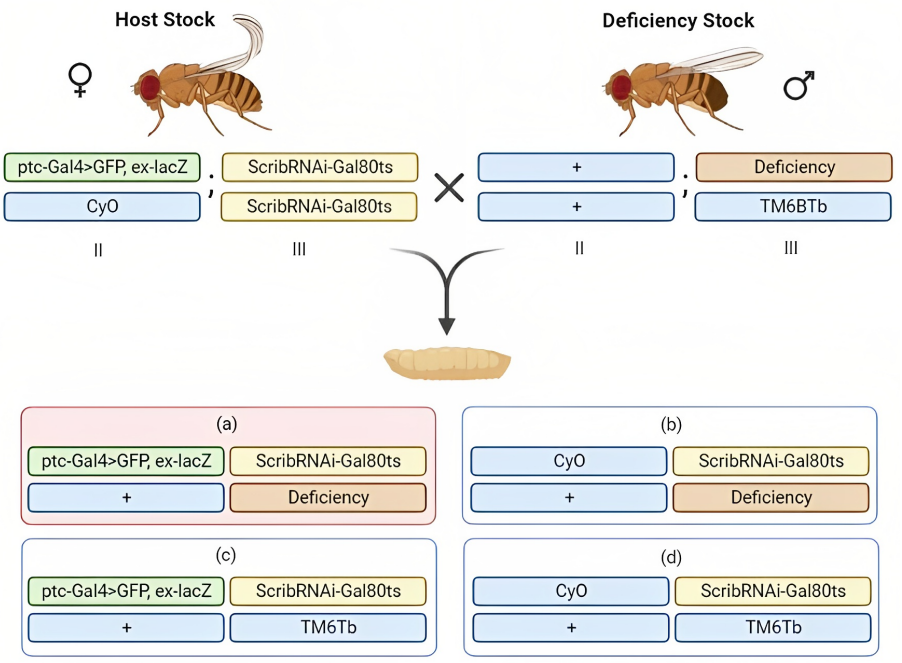

Figure 10. Crosses between the host *scrib* RNAi and Df stocks. The host stock (ptc-Gal4>UAS-GFP, ex-LacZ/CyO; *scrib* RNAi, Gal80^{ts}) is being crossed with the Df stock under Tb balancer. Four genotypic outcomes from the cross are obtained (A-D). (A) The progeny of interest that is taken for imaging. It contains the active *scrib* RNAi, *ptc*-controlled UAS/Gal4, Gal80^{ts}, and the deficiency of interest. (B-D) Progenies are excluded, as they lack vital components: either the deficiency region, or the components of the UAS/Gal4/Gal80^{ts} system. Figure adapted from Fischbach, 2022.

Although the *scrib* RNAi host stock itself has oncogenic properties, our previous study revealed that different dosages of *scrib* have a huge impact on the intensities of oncogenicity (Huang et al., 2022). Thus, in our screening protocol, additional control was employed in a background with one copy of *scrib* (sensitized condition) in addition to a normal positive control with two copies of *scrib*. Sensitized control (one copy *scrib*) is obtained by crossing the host stock with Df 8105 line that is deficient in *scrib* locus and shows severe neoplasia formation in the shorter time (Pos+). Another control (two copies *scrib*) is the self-cross of the host *scrib* RNAi stock that creates a replica of the genotype of the parental flies (Pos). The more precise Pos is heterozygous for the *scrib* RNAi (*ptc*-Gal4, UAS-GFP, ex-LacZ/CyO; *scrib* RNAi, Gal80^{ts}/+), but the control possessing two copies of *scrib* RNAi (homozygous) was used throughout the thesis. Pos allows us to observe the severity of neoplasia under the conditions of a double RNAi-mediated KD, as the host stock has two copies of *scrib* RNAi on the third chromosome (*ptc*-Gal4, UAS-GFP, ex-LacZ/CyO; *scrib* RNAi, Gal80^{ts}/*scrib* RNAi, Gal80^{ts}). This system is used for the comparison of one-copy KD of *scrib*. The

positive-positive control (Pos+) is a sensitised control used for the indirect comparison of the main Df × *scrib* RNAi crosses, as both contain the deficiency regions, the phenotypes of which are comparable (+/+; Df 8105/Tm6B × *ptc*-Gal4, UAS-GFP, ex-LacZ/CyO; *scrib* RNAi, Gal80^{ts}/*scrib* RNAi, Gal80^{ts} → *ptc*-Gal4, UAS-GFP, ex-LacZ/+; *scrib* RNAi, Gal80^{ts}/Df 8105).

Proper experimental crosses require virgin female flies, as mature and inseminated female flies would produce a mixed and incorrect progeny when crossed with male flies from another stock. The identification of the virgin females can be performed with various phenotypic appearances (Figure 11). The most reliable characteristic of the virgin fly is the ventral abdomen spot called meconium (Figure 11A). The virgin flies have a larger body size and brighter dorsal body color (Figure 11B). It is also possible to identify so-called super-virgins (Figure 11C). These are the flies that have just eclosed and can be recognized by unfolded wings.

Figure 11. The phenotypic appearances of the female virgin flies. (A) The ventral view of the female virgin. The dark meconium spot is visible on the lower part of the abdomen (red circle). (B) The dorsal view of the female virgin. The bigger size and brighter colour of the fly are accurate parameters indicating virginity. (C) Examples of female super-virgins. The wings are not yet unfolded. (D) An example of a mature female (left) and male (right) flies.

3.1.3 Temperature shift and conditional KD

After setting up the crosses with Df × *scrib* RNAi (the host stock), Df 8105 (one copy *scrib*) × *scrib* RNAi, and two copies *scrib* RNAi self-cross, dry yeast is added to the vials to facilitate egg laying. Then the vials are placed in a 25°C incubator for 2 days (2D) for the flies to mate before the start of the experiments, subsequently having more progeny. The flies are then transferred to new vials for the 12-hour egg laying at 18°C. The 12-hour period is used for the larvae to be relatively the same age when the sample collection occurs. After 12 hours, the flies are discarded and the vials with eggs are left at an 18°C incubator for 3 days (3D). The subsequent step is the temperature shift, when the developing larvae are transferred to 29°C for another 3D. A total of 6 days after egg laying is required for the larvae to reach the late third instar stage.

The fly progeny with the desired genotype (Figure 10A) expresses GFP in the *ptc* region under the control of UAS-Gal4. The introduction of Gal80^{ts} allows the creation of conditional KD of *scrib* and the subsequent possibility to detect tissue dynamics during early neoplasia formation (Figure 12).

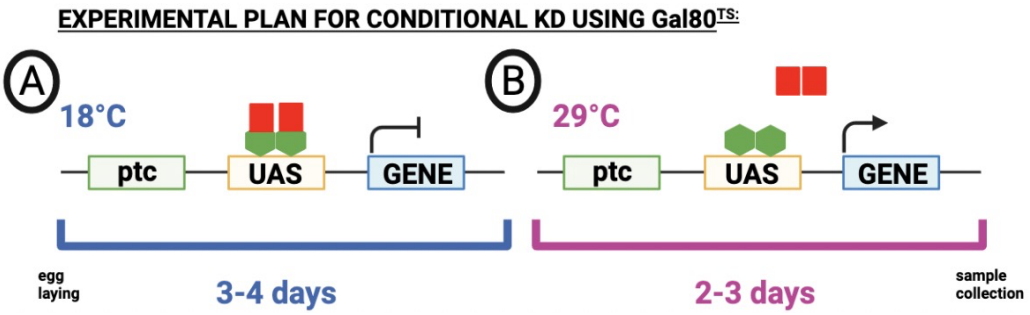

Figure 12. Experimental plan for conditional KD using Gal80^{ts}. (A) The first 3-4 days after egg laying the vials are kept at 18°C. Gal80^{ts} (red) acts as a repressor to Gal4 (green) and the downstream gene is not expressed. (B) Conditional KD of *scrib* occurs during 2-3 days of incubation at 29°C, when Gal80^{ts} becomes inactivated and disassociates from Gal4. The activator role of Gal4 is recovered and the downstream gene is expressed. Figure created with https://biorender.com.

Previous research by Fischbach (2022) proposed various protocols regarding the number of days for flies being kept at different temperatures and the most suitable protocol of 4 days (4D) at 18°C (A) and 2D at 29°C (B) was established. Primary screening in the thesis was conducted under these conditions, although it was noted that they are not suitable after the controls were introduced. Multiple conditions were used to find the most suitable protocol for both controls and the Dfs.

3.1.4 Imaging protocol

3.1.4.1 Preparations and dissection

The sample preparation can be started after the late third instar larvae are obtained while they are wandering on the walls of the vial. Non-Tb larvae are carefully picked up from the vial walls with a thin brush, transferred into a 4-well plate containing 1xPBS (phosphate-buffered saline) solution, and placed on ice to slow down the mobility of larvae. The 4-well plate with larvae is placed under a fluorescent stereomicroscope Leica M205 FA and the salivary glands are checked for the presence of GFP signal. This step allows the identification of GFP positive larvae and decreases the probability of obtaining wing discs without GFP. Preferably ten or more GFP positive larvae are collected and dissected.
The dissection procedure implies the extraction of the wing discs. The procedure takes place under a stereomicroscope on a silicone pad filled with 1xPBS. Larvae are placed into 1xPBS and the posterior part of the body is removed with forceps, so that the wing discs located anteriorly are not damaged. The intestines and most organs are removed until the wing discs are uncovered. The discs bound to the head are carefully transferred into a 1.5 ml Eppendorf tube with 1xPBS until all larvae are dissected.

3.1.4.2 Fixation

Tissue fixation is required for cell preservation and structure integrity. Wing discs are placed in the fixation solution for 20 minutes at room temperature (RT) after removing 1xPBS. The fixation solution consists of formaldehyde (FA) (Sigma-Aldrich®) and 1xPBT (buffer based on PBS and non-ionic detergent Tween 20 (Roche®)) (final concentration 3.7%). Lastly, the FA is removed and the discs are rinsed twice with 1 ml of 1xPBT.

3.1.4.3 Staining

For primary screening, the discs are stained only with DAPI (Thermofisher®, D1306). The concentration of DAPI and staining time can vary and the following conditions were confirmed: 1:300 ratio for 2 hour staining at RT, 1:300 ratio for staining overnight at 4°C, and 1:100 ratio for 30 minute staining at RT. After staining, the DAPI-1xPBT solution is removed and the discs are rinsed twice with 1 ml of 1xPBT with one minute intervals and washed twice with 1xPBT for 10 minutes.

Additional stainings can be performed for the fly lines that showed neoplasia formation. The localization and levels of Yki signal can be measured with the use of polyclonal antibodies staining ex-LacZ product - β-galactosidase, which is a readout for Yki signal (Yu & Pan, 2018). The method used for β-galactosidase staining is a tissue immunostaining, which requires primary and secondary antibodies. The primary antibody used is anti-β-galactosidase (Promega®), and the secondary antibody is anti-mouse Immunoglobulin G (IgG) 568 (Alexa Fluor®). The primary antibody is produced and extracted from mice cell lines, thus the secondary antibody must be related to it for the system to work. The number 568 indicates the wavelength of the light at which the excitement of the secondary antibody is the highest. The 568 wavelength was used as the flies already express GFP. The staining procedure is as follows: the discs are placed in the 5% Goat Serum-PBT blocking buffer (final ratio 1:20) for 2 hours. Anti-β-galactosidase antibody is added to the blocking buffer in 1:100 ratio and the discs are stained overnight at 4°C. The discs are rinsed twice with 1 ml of 1xPBT and washed once with 1xPBT for 10 minutes. The discs are placed in fresh 1xPBT, the anti-mouse 568 antibody is added in the ratio of 1:500 and stained for 2 hours at RT. After staining, the tissues are rinsed and stained with DAPI in the same procedure as discussed before.

3.1.4.4 Wing disc isolation

Stained wing discs are still attached to the anterior part of the larvae and their isolation is required for obtaining proper images during microscopy. The following procedure is performed similar to the dissection. The wing discs are detached from haltere discs and trachea that are bound to them and transferred to 1.5 ml Eppendorf tubes with 1x PBT with a pipette.

3.1.4.5 Mounting

Mounting prepares the stained wing discs for microscopy. The microscopy glass slide and glass cover are cleaned with 70% ethanol and dried with Kimtech® wipes. The wing discs are pipetted on the glass slide and the excess PBT is removed with the wipe. A small amount of mounting solution (either 70% glycerol or commercial mounting medium (Vectashield®)) is added to the discs before the cover glass is placed on top. The excess liquid is then gently removed and the edges are sealed with a transparent nail polish.

3.1.4.6 Microscopy

An Olympus BX51 Fluorescence Microscope with a 20x magnification objective is used for obtaining images. The microscope uses a Hg lamp that allows the fluorescent components of the sample (such as GFP, DAPI, and Alexa 568) to be excited. The images are preferably taken right after mounting, as GFP is pH sensitive. The mounting solution can become acidic over time and the GFP signal can be lost.

3.1.4.7 Image analysis

The analysis of the wing discs is based on the categorized scale, introduced by Fischbach, 2022 (Figure 13). The stage of tissue overgrowth is evaluated by the expansion of the GFP stripe and by the tissue disruption, identifiable with DAPI. The images are colour-adjusted and merged with ImageJ software.

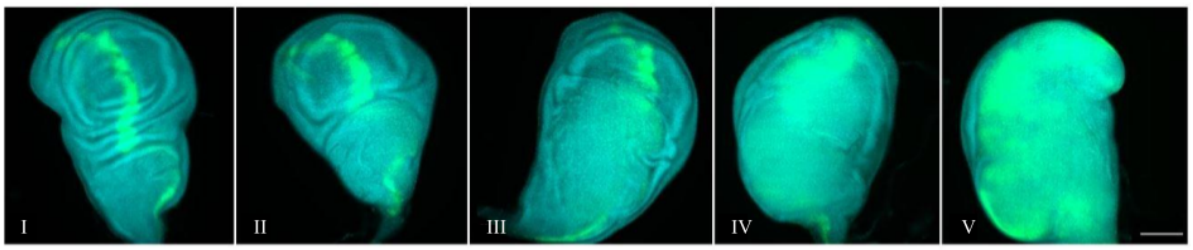

Figure 13. Five stages of tumour progression in the wing discs. The five categories (I-V; left → right) are established to determine the severity of tissue proliferation. The I stage discs have no neoplasia formation and it progresses from stages II to V. The scale (bottom-right) is 100 μm. Adapted from Fischbach, 2022.

3.2 RESULTS

3.2.1 Establishing the protocol for screening

The main reason for the need to change the protocol was that the Pos+ control did not show severe enough phenotype at 2D after temperature shift, thus it was not reliable to correctly identify the real candidate Dfs (Figure 14).

The 3D+3D protocol was then tested. The results showed that the severity of the Pos+ neoplasia phenotype was evident as the majority of the wing discs were type V tumour

according to the proposed scale (Fischbach, 2022), although a small portion of discs still had less severe neoplasia (Figure 14). The behaviour of Dfs was also sufficient (Figure 18). The Pos often showed overproliferation of the tissue and a great spread of GFP signal (Figure 14). Thus, some other variations of days were tested: 3.5D+2D and 3.5D+3D. The results from those screenings showed inconsistent data. For 3.5D+2D, Pos had the predicted phenotype but the severity of neoplasia of Pos+ was not sufficiently strong (Figure 14). For 3.5D+3D, the Pos+ had the predicted neoplasia phenotype, but the Pos started to show higher levels of neoplasia (Figure 14).

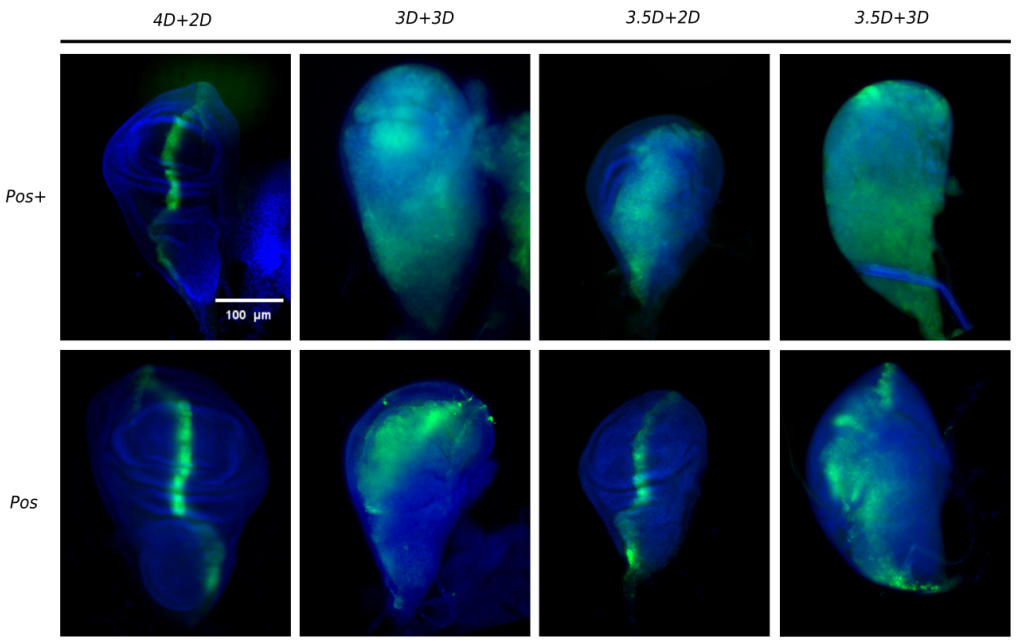

Figure 14. The levels of neoplasia in Pos+ and Pos wing discs under different conditions. The top row represents the disc samples from Pos+ collected during the experiments under varying day conditions. The lower row shows the Pos control samples obtained from different day conditions. 4D+2D Pos+ - no neoplasia, 4D+2D Pos - no neoplasia; 3D+3D Pos+ - severe neoplasia, 3D+3D Pos - medium level of neoplasia; 3.5D+2D Pos+ - medium to severe neoplasia, 3.5D+2D Pos - no neoplasia; 3.5D+3D Pos+ - severe neoplasia, 3.5D+3D Pos - medium level of neoplasia. The scale bar (top-left) is 100 µm.

3.2.2 Primary screening

101 initial lines with deficiency regions on the right arm of the third chromosome were obtained from the BDSC. For this thesis, 10 lines were randomly picked for screening (see Table 2) and swapping of the balancer chromosome was conducted for 4 of them (#1990,

#6962, #7443, and #8029). The lines were screened according to the screening protocol that used 4D at 18°C and 2D at 29°C.

Nine of the lines showed no severe phenotype (Figure 15). According to the established candidate evaluation method by Fischbach (2022), some proportion of wing discs with minor neoplasia in Dfs does not indicate the presence of genes that are as crucial for tissue homeostasis. Thus, these lines were excluded from future secondary screening.

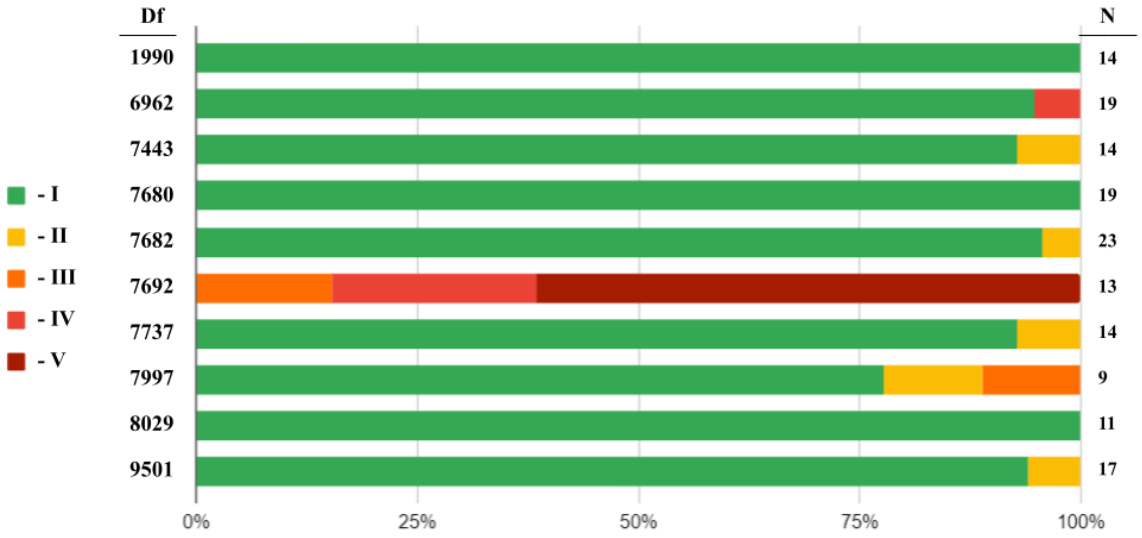

Figure 15. The results of the primary Dfs screening. The figure shows the percentages of the five neoplasia categories in every Df. The phenotypic identification method of the severity of neoplasia was taken from Fischbach (2022). The discs with no neoplasia are represented by green (I), slight tissue overgrowth by yellow (II), medium levels of neoplasia by orange (III), severe tumorigenesis by red (IV), and total ABP loss and tissue disruption/neoplasia by brown (V). The number at the right indicates the total number of wing discs obtained for every Df.

One line, Df 7692, was identified as a potential Df candidate based on the severity of neoplasia phenotype (Figures 15, 16). The proportion of the discs with severe tissue proliferation denotes the potential gene(s) that synergize with Scribble and/or are important for epithelial homeostasis (Figure 15). Besides the spread of GFP signal from the ptc region, DAPI staining showed the disruption of structural integrity in all collected wing discs (Figure 16).

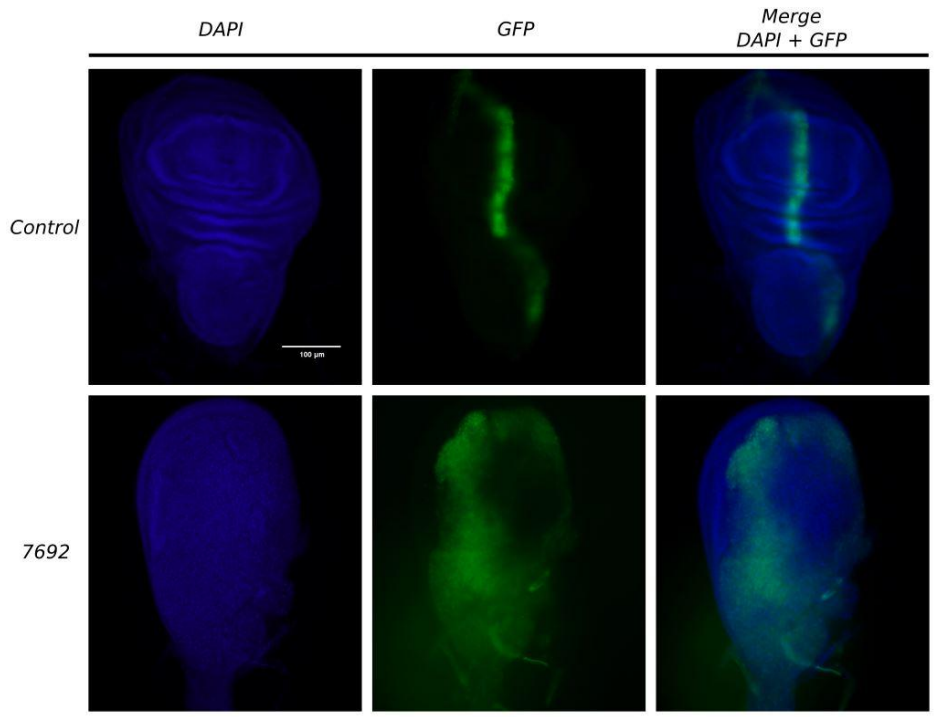

Figure 16. Results of Df 7692 screening. The 7692 deficiency line (lower panels) showed severe levels of neoplasia formation compared to the control (upper panels). The DAPI staining (left), the GFP expression in the *ptc* region (middle), and the merged channels (right) are presented. The host *scrib* RNAi stock was used as a control. Control N=11, Df 7692 N=10. The scale bar (top-left) is 100 µm.

The deleted region of the Df 7692 consists of 21 genes. Six of the genes functionally remained unknown (Table 3).

According to the severity categorization by Fischbach (2022), the Df line 7692 belongs to the IV category of severity (see Figure 13).

Table 3. Deleted genes in the Df 7692.

Gene abbreviation	Known information
sima	Molecular functions: enables RNA polymerase II transcription regulatory region sequence-specific DNA binding and protein dimerization activity. Molecular functions: involved in negative regulation of cell growth, regulation of cell migration, positive regulation of transcription by RNA polymerase II, insulin receptor signaling pathway, oogenesis, positive regulation of autophagy, regulation of innate immune response, and trachea development.
lncRNA:CR46112	Molecular and biological functions are unknown.

CG45072	Molecular and biological functions are unknown.
CG45073	Molecular and biological functions are unknown.
Ppi1	Molecular function: enables protein phosphatase 1 binding. Biological functions are unknown.
CG31029	Is expressed in spermatozoon. Molecular and biological functions are unknown.
Tpi	Molecular functions: enables protein homodimerization and triose-phosphate isomerase activity. Biological functions: involved in determination of adult lifespan, gluconeogenesis, nervous system process, and response to mechanical stimulus.
AdoR	Molecular function: enables G protein-coupled adenosine receptor activity. Biological functions: involved in adenylate cyclase-activating G protein-coupled receptor signaling pathway, chemical synaptic transmission, negative regulation of calcium ion import, and regulation of carbohydrate metabolic process.
asRNA:CR46082	Molecular and biological functions are unknown.
CG15529	Molecular function: enables signaling adaptor activity. Biological functions: predicted to be involved in intracellular signal transduction and transmembrane receptor protein tyrosine kinase signaling pathway.
CG11498	Molecular function is unknown. Biological functions: predicted to be involved in mitochondrial protein catabolic process and mitophagy by induced vacuole formation. Predicted to be active in mitochondrial outer membrane. Is expressed in spermatozoon.
VhaAC45RP	Molecular function: enables ATPase regulator activity. Biological functions: involved in synaptic vesicle lumen acidification and regulation of cellular pH.
Rsod	Molecular functions: predicted to enable metal ion binding and superoxide dismutase activity. Biological function: involved in superoxide metabolic process.
Mlc2	Molecular functions: enables calcium ion binding and myosin heavy chain binding. Biological functions: involved in flight, muscle system process, myofibril assembly, locomotion, and post-embryonic development.
CG1983	Molecular function: predicted to enable pyridoxal phosphate binding. Biological function is unknown.
CG15530	Molecular and biological functions are unknown.

Bet5	Molecular function: predicted to contribute to guanyl-nucleotide exchange factor activity. Biological functions: predicted to be involved in endoplasmic reticulum to Golgi vesicle-mediated transport, Golgi vesicle transport, and vesicle-mediated transport.
lncRNA:CR44262	Molecular and biological functions are unknown.
CG9747	Molecular functions: predicted to enable iron ion binding, oxidoreductase activity, and stearoyl-CoA 9-desaturase activity. Biological functions: predicted to be involved in lipid metabolic process and unsaturated fatty acid biosynthetic process.
CG15531	Molecular functions: predicted to enable iron ion binding, oxidoreductase activity, and stearoyl-CoA 9-desaturase activity. Biological functions: predicted to be involved in lipid metabolic process and unsaturated fatty acid biosynthetic process.
CG9743	Molecular functions: predicted to enable iron ion binding, oxidoreductase activity, and stearoyl-CoA 9-desaturase activity. Biological functions: predicted to be involved in lipid metabolic process and unsaturated fatty acid biosynthetic process.

3.2.3 Secondary screening

The Df 8069 was previously identified as a candidate Df and was chosen for a finer screening (Fischbach, 2022). Collection of the Bloomington Stock Center deficiency lines provides with 15 stocks that overlap with the 8069 line. 14 of them were ordered, the balancer chromosome swapping was performed, and then 9 lines were screened (Table 4; Figures 17, 18).

Table 4. Dfs used for the Df 8069 candidate secondary screening. The table shows the Df lines used, their starting and ending points of deleted regions, the length of the deletion, and the number of deleted genes.

Df	Starting point (nt)	Ending point (nt)	Deletion length (nt)	Number of genes (n)
8069 (candidate)	11 587 040	12 408 601	821 561	158
BSC675 (26527)	11 491 583	11 691 527	199 944	57
BSC727 (26579)	11 715 150	12 081 822	366 672	64
BSC676 (26528)	11 789 484	12 203 981	414 497	81
BSC458 (24962)	11 938 467	12 203 981	265 514	55
BSC840 (29024)	11 956 819	12 111 238	154 419	20
Exel6116 (7595)	12 081 855	12 203 981	122 126	28
BSC396 (24420)	12 111 239	12 136 461	25 222	11
BSC730 (26828)	12 162 977	12 843 324	680 347	90
ED4483 (8070)	12 277 220	12 693 214	415 994	54

Four lines that covered the larger parts of the candidate line 8069 were initially taken for the screening to narrow down the genomic region: Df 26527, Df 26579, Df 24962, and Df 26828. The obtained results allowed to exclude 5 Dfs without screening them, as the deficiency regions from these lines overlap with those that showed no proliferative phenotype during screening. Thus, it was possible to confirm that those Dfs do not contain gene(s) involved in ABP homeostasis together with Scrib.

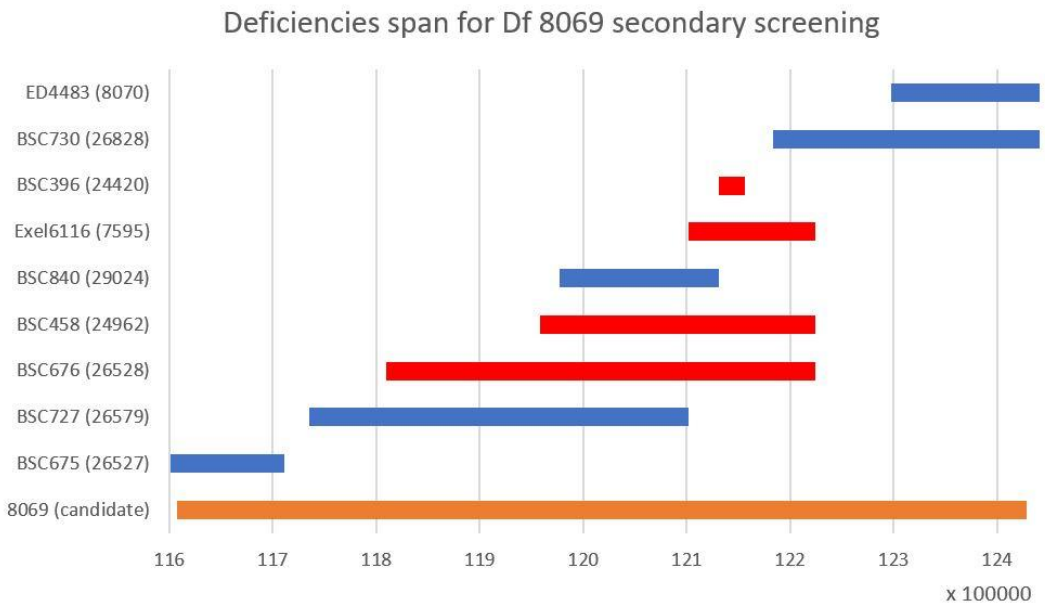

Figure 17. Genomic region of the candidate Df 8069 with the overlapping Dfs. Fifteen Dfs have the overlapping regions with the candidate line that allow the finer screening of the candidate. Out of 9 screened lines, 5 showed no-neoplasia (blue) and 4 showed strong neoplasia (red) phenotypes. The candidate Df 8069 is marked with orange.

Dfs 26528, 24962, 7595, and 24420 showed high levels of neoplasia (Figures 17, 18). Several lines that showed no neoplasia have overlapping regions with the lines with the neoplasia phenotype. By excluding those overlapping genomic regions, it was further possible to narrow down the region even more.

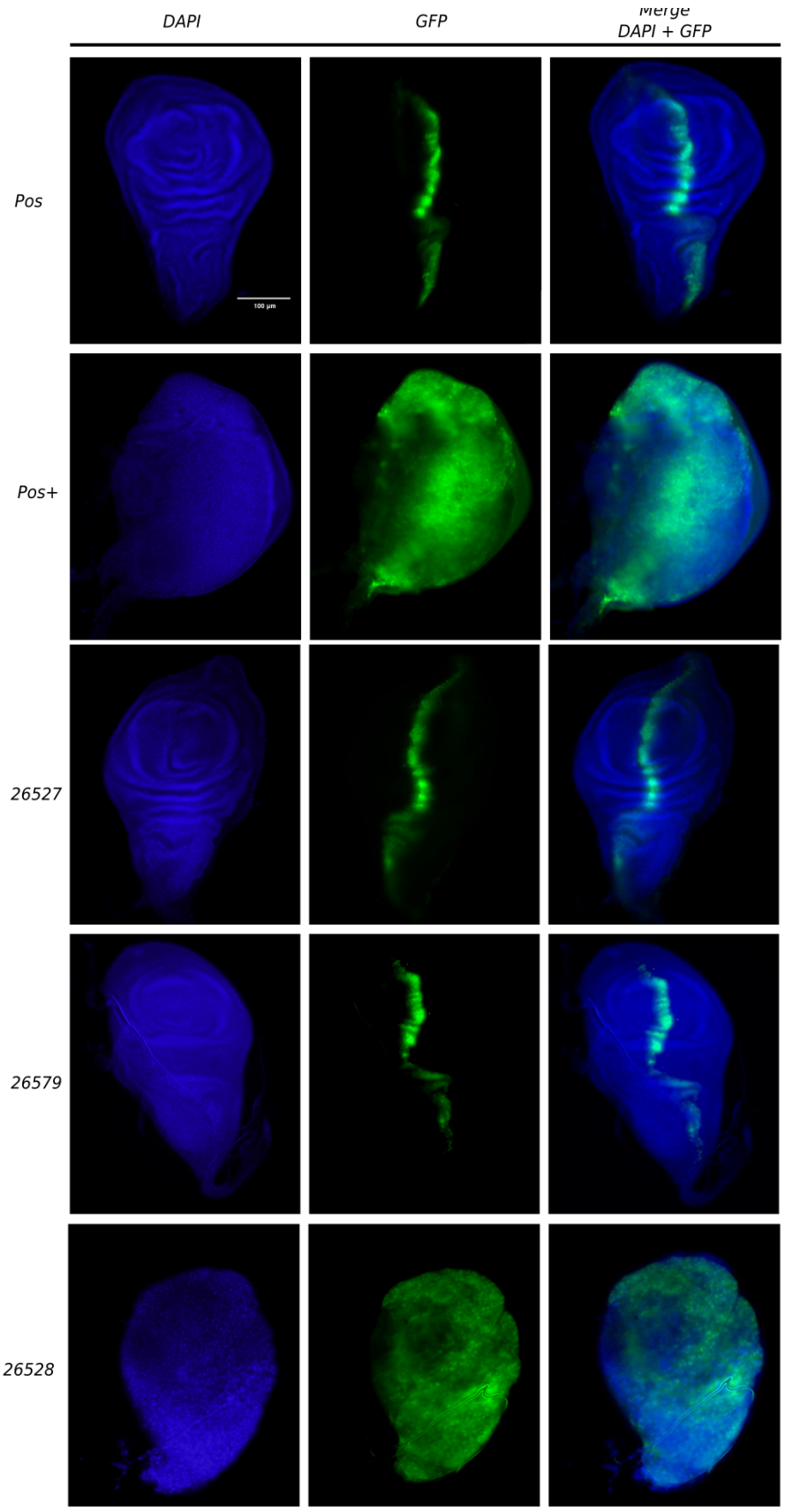
DAPI
GFP
Merge
DAPI + GFP
Pos
Pos+
26527
26579
26528
100 µm

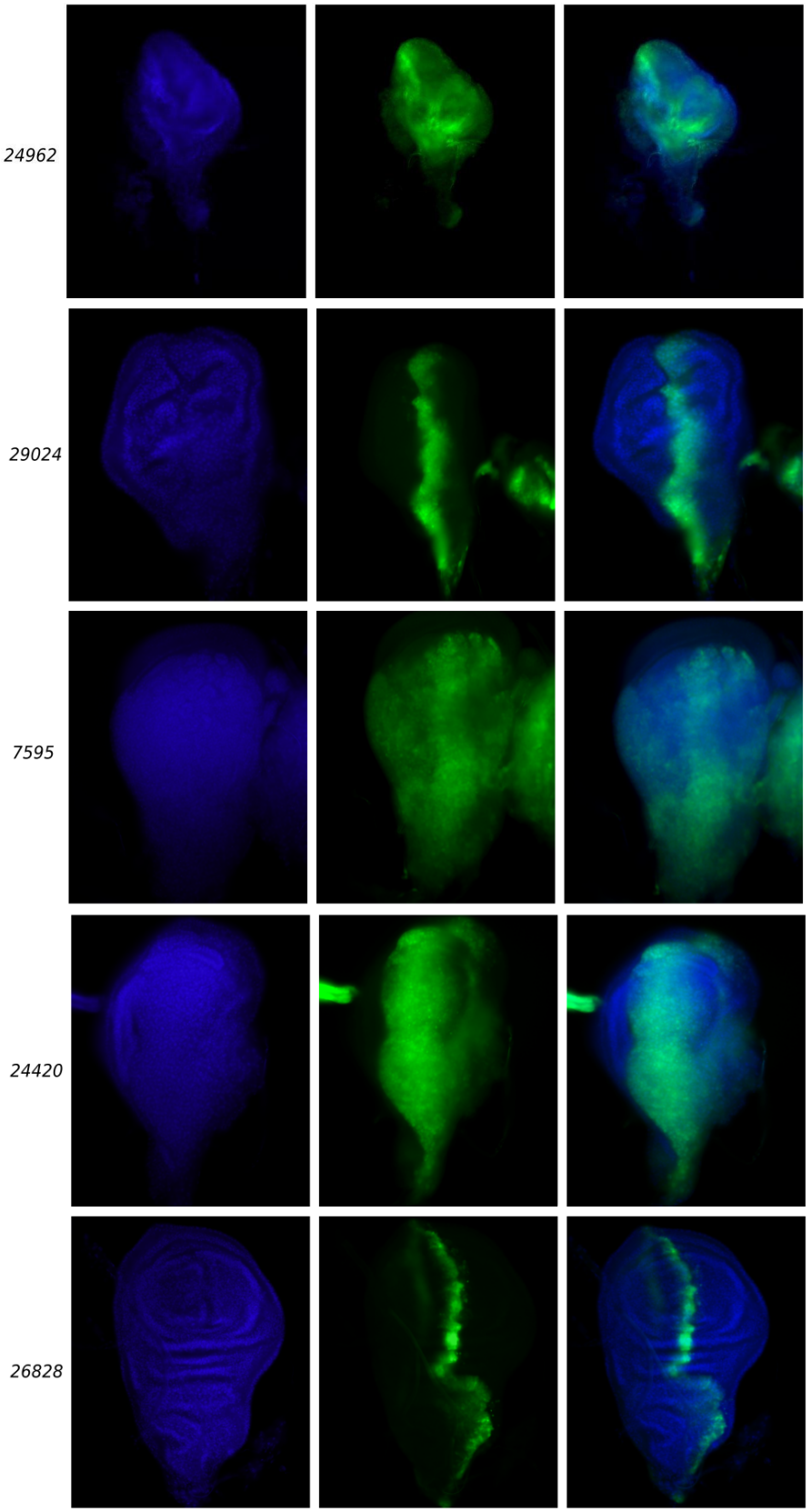
24962
29024
7595
24420
26828

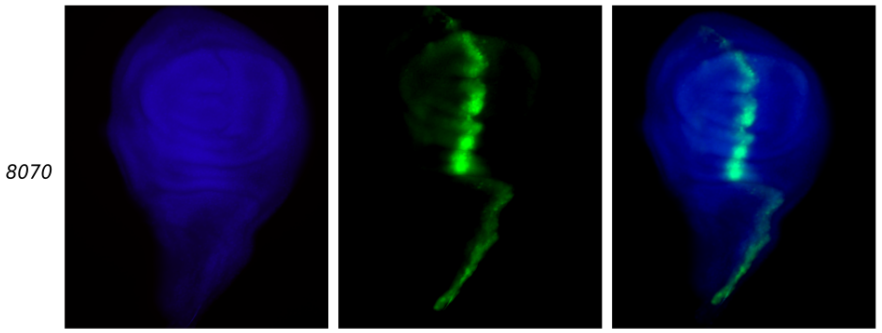

Figure 18. Secondary screening results. Lines 26528, 7595, 24420, and 24962 showed neoplasia phenotype. Positive (first upper panels) and positive-positive (second upper panels) controls are used to determine that the protocol is robust. The staining with DAPI (left), the GFP expression (middle), and the merge of two channels (right) are presented. The host *scrib* RNAi stock was used as a Pos control and the Df 8105 × *scrib* RNAi host stock cross was used as a Pos+ control. The scale bar (top-left) is 100 μm.

Eventually, it was possible to identify 52 kilobases of DNA that might contain a gene of interest that is located between the end of Df 29024 deletion and the beginning of Df 26828 deletion. Overall, the identified region contains 18 genes (Table 5).

Table 5. Deficient genes in the obtained region.

Gene abbreviation	Known information
vers	Biological functions: involved in regulation of stem cell differentiation and positive regulation of DNA-templated transcription.
ssp	Molecular functions: enables beta-catenin and DNA binding. Biological functions: involved in positive regulation of DNA endoreduplication, DNA-templated transcription, and imaginal disc growth.
CG11560	Molecular function: predicted to enable DNA binding. Biological function: predicted to be involved in positive regulation of DNA-templated transcription.
yps	Molecular functions: enables binding of protein, mRNA, and nucleic acid. Biological functions: involved in mRNA splicing via spliceosome, oogenesis, and regulation of gene expression.
Ir68b	Molecular function: predicted to enable ligand-gated monoatomic ion channel activity. Biological function: predicted to be involved in detection of chemical

	stimulus.
CG34241	Molecular and biological functions are unknown.
asRNA:CR11538	Molecular functions: enables protein sequestering and transcription regulator inhibitor activity. Biological functions: involved in negative regulation of antimicrobial peptide production and Toll signaling pathway.
Lsp2	Biological functions: involved in motor neuron axon guidance and synaptic target inhibition.
DEF8	Is expressed in organism. Orthologous to human DEF8. Molecular and biological functions are unknown.
asRNA:CR45892	Molecular and biological functions are unknown.
CG5645	Biological function: predicted to be involved in endonucleolytic cleavage in ITS1 to separate SSU-rRNA from 5.8S rRNA and LSU-rRNA from tricistronic rRNA transcript.
Atg12	Molecular functions: enables protein tag and contributes to Atg8 ligase activity. Biological functions: involved in autophagy, cellular response to starvation, glycophagy, larval midgut cell apoptosis, and macroautophagy.
ND-SGDH	Biological functions: involved in determination of adult lifespan, response to reactive oxygen species (ROS), and mitochondrial respiratory chain complex I assembly.
RhoGAP68F	Molecular function: enables GTPase activator activity. Biological functions: involved in imaginal disc-derived leg morphogenesis, negative regulation of endocytic recycling and stress fiber assembly, positive regulation of synaptic assembly at neuromuscular junction, Rho protein signal transduction, and signal transduction.
elF3I	Molecular function: enables translation initiation factor activity. Biological function: involved in translational initiation.
Nrx-IV	Biological functions: involved in cell-cell junctions, protein localization, axon ensheathment, dorsal closure, establishment of glial blood-brain barrier, nerve maturation, heart process, presynaptic membrane assembly, regulation of tube size, open tracheal system, septate junction assembly, synaptic target recognition, and terminal button organization.
CG32099	Molecular functions: predicted to enable holo-[acyl-carrier-protein] synthase activity and magnesium ion binding. Biological function: predicted to be involved in lysine biosynthetic process via aminoadipic acid.
CG9760	Molecular and biological functions are unknown.

It is important to denote that the total number of collected wing discs in 3 Df samples (#8070, #7595, and #24420) is statistically insufficient to obtain a complete picture of the gene significance in the deleted region as the number of collected wings was less than 6 (Figure 19).

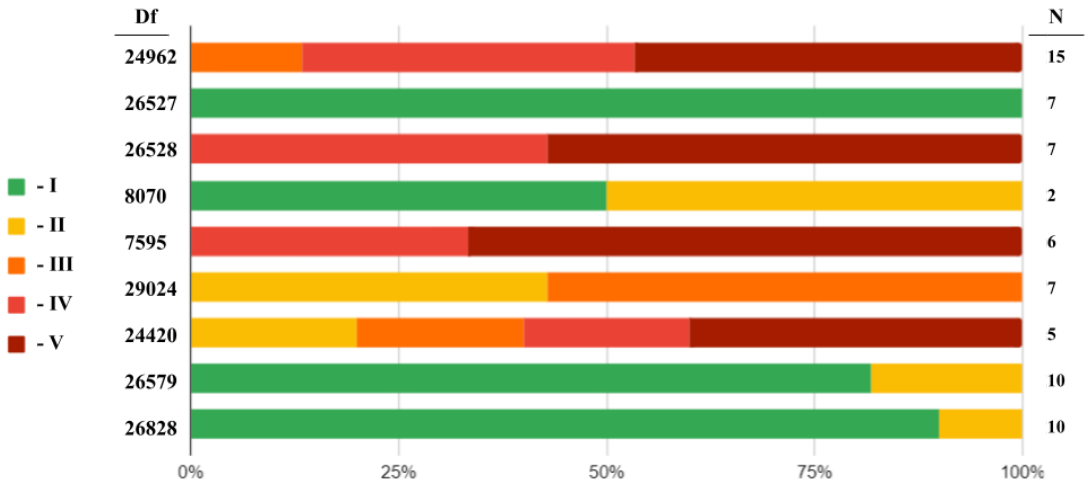

Figure 19. The results of the secondary Dfs screening. The figure shows the percentages of five neoplasia categories in every Df. The phenotypic identification method of the severity of neoplasia was taken from Fischbach (2022). Green (I) represents the discs with no neoplasia, yellow (II) - slight tissue overgrowth, orange (III) - medium levels of neoplasia, red (IV) - severe tumorigenesis, and brown (V) - total ABP loss and tissue disruption/neoplasia. N (top-right) denotes the total number of wing discs obtained for every Df.

Nevertheless, using a gene map and relying on the genomic location of deletions, the results from screenings of other Dfs can be used to confirm whether those lines contain genes that are involved in ABP maintenance in cooperation with Scrib. However, the proper confirmational screening of those lines must be done in the future.

The contents of the region of interest were studied and one possible candidate gene was identified - *neurexin-IV* (*nrx-IV).* The screening of *nrx-IV* RNAi lines on the second and third chromosomes were performed (Figure 20). The mutant *nrx-IV* allele stock (amorphic / hypomorphic) was also screened for a better understanding of whether Nrx-IV has a synergy with Scrib in the context of ABP homeostasis (Figure 20). An additional staining with anti-β-galactosidase was performed to be able to see the Yki signal in the wing discs.

The results show slightly variable phenotypes between the two RNAi lines (Figure 20). On one hand, the spread of GFP across the tissue and the levels of tissue overgrowth indicated by DAPI staining are equally severe. On the other hand, the Yki signal in the *nrx-IV* RNAi III

line dominates over the other *nrx-IV* lines (Figure 20). This indicates that Yki activity depends on the genomic location where the RNAi mechanism is primarily located.

A negative control (*ptc*-Gal4; Tub-Gal80^{ts}, UAS-Tub-mCherry crossed with *nrx-IV* RNAi III) was used for the experiments with the *nrx-IV* lines to see the behaviour of the alleles without the KD of *scrib* (Figure 20). In the negative control, the red stripe in the *ptc* region represents the mCherry signal and indicates no overproliferative phenotype (Figure 20).

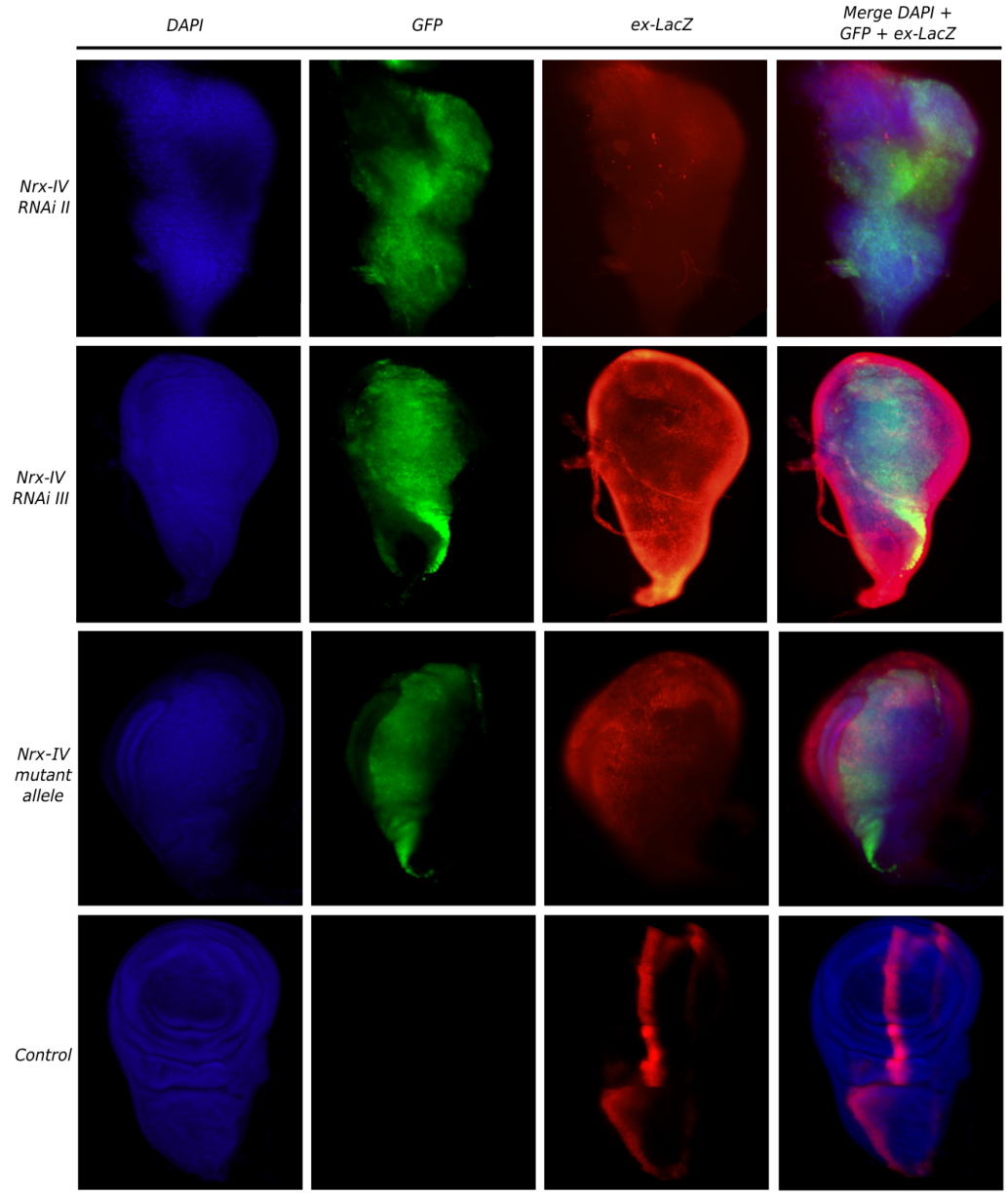

Figure 20. Screening of *nrx-IV* as a candidate gene. The emphasis was made on *nrx-IV* and 3 fly lines were screened: two *nrx-IV* RNAi lines (first and second upper panels) and the line possessing *nrx-IV* mutant allele (third panels). *Nrx-IV* RNAi II showed structural disruptions of the wing discs and low levels of Yki signal. *Nrx-IV* RNAi III showed similar levels of neoplasia, but a more intense Yki signal. *Nrx-IV* mutant allele showed moderate overproliferation and Yki signal propagation. *nrx-IV* RNAi III × *ptc*-Gal4; Tub-Gal80^{ts}, UAS-Tub-mCherry was used as a negative control. *nrx-IV*

RNAi II N=7, *nrx-IV* RNAi III N=11, *nrx-IV* mutant N=10, control N=11. The scale bar (top-left) is 100 μm.

3.3 DISCUSSION

The screening of the fly lines deficient in specific genomic regions allows us to identify genes that are involved in the maintenance and/or establishment of apico-basal polarity (ABP) and epithelial tissue homeostasis together with Scrib (Fischbach, 2022). The loss of ABP eventually leads to tissue structure disruption and neoplasia formation (Enomoto & Igaki., 2011). Identification of such genes is decisive for understanding the mechanisms required for the proper intercellular alignment, cell communication, and epithelial morphogenesis (Huang et al., 2023).

In both primary (3R) and secondary (3L) screenings, we can affirm that the novel Df screening method is robust and well-established. The method can be used to find potential candidate genes by using multiple overlapping Dfs. The deleted genomic regions that do not show neoplasia phenotype can be excluded and regions with phenotype can be screened and examined further.

To resolve the issue with both positive-positive (Pos+) and positive (Pos) controls and to have a better working protocol for the ongoing screening, one possible suggestion is to introduce changes into temperature conditions, rather than the number of days. For instance, the initial incubation at 18°C could be changed to 19°C. In addition, the 29°C conditions at which the conditional KD occurs could also be changed and switched to lower temperatures (27-28°C). It would be possible to examine the behaviour of all the fly lines under variable conditions and establish a proper and robust 3D+3D protocol. However, the screening using the 4D+2D protocol is more reliable to identify the presence of important genes, as the 3D+3D protocol has a higher probability to give false positive results. Thus, additional testing of the 4D+2D protocol under variable conditions can be arranged simultaneously with the 3D+3D protocol and the collected data can then be analyzed. By comparing and contrasting different day and temperature conditions that would change the time of organism development and the progression of neoplasia formation after the KD of *scrib* would make it possible to choose the most appropriate protocol and apply it for future screenings.

Another possible solution to overcome the problem is to change the logic of the positive control. Pos was mainly used to evaluate the severity of tissue overproliferation mediated by double KD of *scrib*. It is rather a useful control, as it is possible to use the obtained data to

compare the more severe double KD with a KD with one copy of *scrib* RNAi and use it for the creation of a proper and updated protocol. One issue with Pos is that it is not possible to compare it with the Df experiments due to the fact that the desired progeny of Df × *scrib* RNAi cross reflects the phenotype of both the deficiency and RNAi (Figure 10a). The progeny from the self-cross of the host stock obtains two copies of *scrib* RNAi and it is impossible to properly compare the results without the effects of deficiency. Double RNAi KD is phenotypically distinct from the RNAi/Df, because the effects of double RNAi KD are known and well-established. The presence of deficiency regions in addition to one-copy RNAi would introduce different effects on cellular level and subsequent variation in phenotypes, depending on the contents of the deleted genomic region. Thus, it is possible to use another Pos for the experiments that would correlate to the one copy RNAi KD - an excluded progeny from the Df × *scrib* RNAi cross (Figure 10c). A half of the progeny from the cross of Df with *scrib* RNAi obtains all the required components for both UAS/Gal4/Gal80^{ts} system and conditional KD on the second and third chromosomes. Such a progeny that also obtained Tm6B balancer could be used instead of the two-copy RNAi KD that was used as a reference in the thesis. Moreover, the larvae from that progeny have the Df background, as they were collected from the Df × host stock cross, which would intensify the correlation between the control and the deficiency line of interest. The selection of such a progeny can be done in the same way as the selection of the sample larvae for the deficiency region screening, but only larvae showing Tb phenotype would be selected as the control.

The primary screening of 10 candidate lines with deletions in the right arm of the third chromosome presented important data about the regions that do and do not contain the possible important genes for ABP homeostasis together with Scrib. The identified Df 7692 showed high levels of neoplasia (Figure 16). Therefore, 9 of the screened lines that did not show a neoplasia phenotype can be excluded and only the line 7692 will be used for the secondary screening. Df 7692 contains a short deletion region that contains 21 genes, of which the functions of 6 are still not known. For now it is possible to turn more attention to two of the genes in the line: *CG15529* and *Mlc2*. *CG15529* is predicted to be involved in intercellular signal transduction and *Mlc2* is expressed in wing imaginal discs (https://flybase.org). Even though these genes may have synergy with Scrib in the context of neoplasia formation, it is important to note that it is not possible to exclude the other genes. Even though the known functions of these genes do not correlate to the described system, it is impossible to predict if or how they interact with Scrib and therefore are not associated with the ABP homeostasis or maintenance. Df 7692 has only one overlap with the other line - Df 25006. The screening of Df 25006 would allow us to identify the possible importance of 6

genes, which are located in the overlapping area. From these results (6 genes) we could exclude them if they do not show neoplasia phenotype. On the other hand, if the Df 25006 does not have a neoplasia phenotype, further RNAi screening with the genes in the region will be performed. If Df 25006 shows the tumourous phenotype, the RNAi lines for the genes will also be used.

The finer screening of previously identified Df 8069 (Fischbach, 2022) enabled us to narrow down the region of 18 genes. They are located between the end of Df 29024 deletion and the beginning of Df 26828 deletion (Figure 17). The functions of 3 genes located in the region are not known. It could be seen that one small region of the candidate line is not covered by any shorter Dfs. It is genomically located between the deletions of Df 26527 and Df 26579 and contains 8 genes (Figure 17). Nonetheless, the exclusion of this small region does not introduce any bias to the overall picture, because the region containing genes important for ABP homeostasis was identified in this thesis using the results of other Dfs. It is possible to perform the screening of Df 8068 to cover the missed region and obtain the confirmational data. Nevertheless, as the secondary screening enabled us to identify a shorter region of interest based on the neoplasia phenotype, the screening of the previously mentioned Df would be unnecessary.

The genes from the identified region were studied and several potential candidate genes were found: *Nrx-IV, RhoGAP68F, ssp,* and *yps*. *Nrx-IV* is a core protein of SJs, *RhoGAP68F* is involved in epithelial morphogenesis, *ssp* contributes to regulation of wing disc growth, and *yps* regulates gene expression (https://flybase.org/). These genes will be the initial targets for the future screening, but as discussed previously, it is impossible to exclude other 14 genes and they will also be studied in the future as secondary candidates.

One of the potential gene candidates, *nrx-IV*, was also screened both by using RNAi and mutant allele fly lines. From the results we found that the spread of GFP signal indicates some levels of importance of Nrx-IV in epithelial polarity and early neoplasia formation (Figure 20). Moreover, to additionally confirm our hypothesis that Nrx-IV might be important in the context of ABP, we used ex-LacZ staining, which is a readout for Yki signal, and we found that Yki signal was detectable across the whole area of imaginal discs (Figure 20). The variability of the Yki signal between the two RNAi lines suggests that the intensity of Yki is dependent on the location of the UAS-RNAi insertion in the genome, as different chromosomal regions are transcribed at different rates. Nevertheless, this hypothesis must be further investigated.

The *nrx-IV* mutant allele screening showed slightly variable phenotypes among the obtained samples. The data obtained from BDSC specifies that the line used for the screening can be

amorphic and hypomorphic simultaneously, thus both a loss-of-function (LOF) allele that produces no active protein and alleles with only a partial LOF in flies were present in the stock. That might explain the variability of the phenotypes obtained during screening, yet it is barely noticeable.

The continuation of the project will involve the screening of the genes that were identified during this thesis. Other candidates, identified by Fischbach (2022), will also be screened in the search of additional candidate genes that contribute to the establishment of ABP through homeostasis with Scrib. The primary screening of other Dfs from the right arm of the third chromosome will be performed and the newly identified candidates will be studied during the secondary screening. When all the important genes from the third chromosome are identified, it will be possible to use the BDSC deficiency toolkit to screen the second chromosome of *Drosophila*.

One important aspect to mention is that the main concern of the whole project is not solely focused on the wing disc development alone. The main goal is to obtain a deeper understanding of Scrib and to use the data onwards to broaden the knowledge of human cancer research, as there are several cancer types associated with human *SCRIB* (Santoni et al., 2020).

The *nrx-IV* candidate gene, identified throughout this thesis has a human ortholog, which is associated with Pitt-Hopkins-like syndrome - CNTNAP2 (https://flybase.org/). The confirmation of *nrx-IV* and further investigation of the important genes to be involved in homeostasis with Scrib and their involvement in ABP preservation would contribute to human cancer research and allow the creation of treatments for various human carcinoma types.

SUMMARY

The fundamental goal of the thesis was to locate genomic regions that contain candidate genes that are involved in the establishment and/or maintenance of ABP and tissue homeostasis together with Scribble. In the thesis the UAS/Gal4/Gal80^{ts} system was used to perform the conditional KD of *scrib* by RNAi in the ptc region of *Drosophila* wing imaginal disc.

The primary screening enabled us to exclude 9 regions with the total number of 622 genes and to find an appropriate candidate (Df 7692) that contains 21 genes that will be studied in the future.

The secondary screening of larger and shorter deletion regions was performed with variable protocol conditions. The results suggest that the Nrx-IV, one of the core components of septate junctions, has a moderate importance for the ABP maintenance. Nevertheless, the results from Df 8069 secondary screening imply the involvement of some other genes closely located to the *nrx-IV* in the genome. By using additional Dfs or candidate gene RNAi lines, further screening and investigation into the genome is needed to properly understand which genes are involved in the establishment and/or maintenance of ABP as there are still many unanswered questions. Through this knowledge it is possible to understand the so far unknown mechanisms that are needed for proper epithelial tissue development.

Through the work done in the thesis, it is possible to confirm that the 3 days at 18°C and 3 days at 29°C protocol has the most suitable conditions. Nevertheless, the change of the positive control and additional examination of protocols with variable day and temperature conditions is required to be able to create a robust protocol for the ongoing screenings.

REFERENCES

Adams, M. R., Celniker, S. E., Holt, R. J., Evans, C., Gocayne, J. D., Amanatides, P., Scherer, S. W., Li, P. R., Hoskins, R. A., Galle, R., George, R., Lewis, S. R., Richards, S., Ashburner, M., Henderson, S. N., Sutton, G. C., Wortman, J. R., Yandell, M., Zhang, Q., . . . Venter, J. C. (2000). The Genome Sequence of *Drosophila melanogaster*. *Science*, *287*(5461), 2185–2195. https://doi.org/10.1126/science.287.5461.2185

Aegerter-Wilmsen, T., Aegerter, C. M., Hafen, E., & Basler, K. (2007). Model for the regulation of size in the wing imaginal disc of *Drosophila*. Mechanisms of Development, 124(4), 318–326. https://doi.org/10.1016/j.mod.2006.12.005

Ahmad, M., Chaudhary, S. U., Afzal, A. J., & Tariq, M. (2015). Starvation-Induced Dietary Behaviour in *Drosophila melanogaster* Larvae and Adults. *Scientific Reports*, *5*(1). https://doi.org/10.1038/srep14285

Apidianakis, Y., & Rahme, L. G. (2011). *Drosophila melanogaster* as a model for human intestinal infection and pathology. *Disease Models & Mechanisms*, *4*(1), 21–30. https://doi.org/10.1242/dmm.003970

Ashburner, M., Misra, S., Roote, J., Lewis, S. E., Blazej, R., Davis, T., ... & Rubin, G. M. (1999). An exploration of the sequence of a 2.9-Mb region of the genome of *Drosophila melanogaster*: the Adh region. *Genetics*, 153(1), 179-219. https://doi.org/10.1093/genetics/153.1.179

Badouel, C., & McNeill, H. (2009). Apical junctions and growth control in *Drosophila*. *Biochimica Et Biophysica Acta - Biomembranes*, *1788*(4), 755–760. https://doi.org/10.1016/j.bbamem.2008.08.026

Barreda, D., Gutiérrez-González, L. H., Martínez-Cordero, E., Cabello-Gutiérrez, C., Chacón-Salinas, R., & Santos-Mendoza, T. (2020). The Scribble Complex PDZ Proteins in Immune Cell Polarities. *Journal of Immunology Research*, *2020*, 1–12. https://doi.org/10.1155/2020/5649790

Barwell, T., DeVeale, B., Poirier, L., Zheng, J., Seroude, F., & Seroude, L. (2017). Regulating the UAS/GAL4 system in adult *Drosophila* with Tet-off GAL80 transgenes. *PeerJ*, *5*, e4167. https://doi.org/10.7717/peerj.4167

Beira, J. V., & Paro, R. (2016). The legacy of *Drosophila* imaginal discs. *Chromosoma*, *125*(4), 573–592. https://doi.org/10.1007/s00412-016-0595-4

Bellen, H. J., Tong, C., & Tsuda, H. (2010). 100 years of *Drosophila* research and its impact on vertebrate neuroscience: a history lesson for the future. *Nature Reviews Neuroscience*, *11*(7), 514–522. https://doi.org/10.1038/nrn2839

Brand, A. H., & Perrimon, N. (1993). Targeted gene expression as a means of altering cell fates and generating dominant phenotypes. *Development*, *118*(2), 401–415. https://doi.org/10.1242/dev.118.2.401

Campanale, J. P., Sun, T. Y., & Montell, D. J. (2017). Development and dynamics of cell polarity at a glance. *Journal of Cell Science*, *130*(7), 1201–1207. https://doi.org/10.1242/jcs.188599

Canales Coutiño, B., Szamek, E., Markus, Z., & Georgiou, M. (2021). Generation and live imaging of tumors with specific genotypes in the living fly pupa. *STAR Protocols*, *2*(3), 100672. https://doi.org/10.1016/j.xpro.2021.100672

Cao, F., Miao, Y., Kedong, X., & Li, J. (2015). Lethal (2) Giant Larvae: An Indispensable Regulator of Cell Polarity and Cancer Development. *International Journal of Biological Sciences*, *11*(4), 380–389. https://doi.org/10.7150/ijbs.11243

Chen, C. C., Gajewski, K. M., Hamaratoglu, F., Bossuyt, W., Sansores-Garcia, L., Tao, C., & Halder, G. (2010). The apical-basal cell polarity determinant Crumbs regulates Hippo signaling in *Drosophila*. *Proceedings of the National Academy of Sciences of the United States of America*, *107*(36), 15810–15815. https://doi.org/10.1073/pnas.1004060107

Choudhary, S., Lee, H. H., Maiti, M., He, Q., Cheng, P., Liu, Q., & Liu, Y. (2007). A Double-Stranded-RNA Response Program Important for RNA Interference Efficiency. *Molecular and Cellular Biology*, *27*(11), 3995–4005. https://doi.org/10.1128/mcb.00186-07

De Lorenzo, C., Strand, D., & Mechler, B. M. (1999). Requirement of *Drosophila* I(2)gl function for survival of the germline cells and organization of the follicle cells in a columnar epithelium during oogenesis. *The International Journal of Developmental Biology*, *43*(3), 207–217. http://www.ijdb.ehu.es/web/paper.php?doi=10410900

De, O., Rice, C., Zulueta-Coarasa, T., Fernandez-Gonzalez, R., & Ward, R. E. (2022). Septate junction proteins are required for cell shape changes, actomyosin reorganization and cell adhesion during dorsal closure in *Drosophila*. *Frontiers in Cell and Developmental Biology*, *10*. https://doi.org/10.3389/fcell.2022.947444

Deolankar, S. C., Najar, M. A., Raghu, S. V., & Prasad, T. S. K. (2022). Aβ42 Expressing *Drosophila melanogaster* Model for Alzheimer's Disease: Quantitative Proteomics Identifies Altered Protein Dynamics of Relevance to Neurodegeneration. *Omics a Journal of Integrative Biology*, *26*(1), 51–63. https://doi.org/10.1089/omi.2021.0173

Diaz De La Loza, M., & Thompson, B. (2017). Forces shaping the *Drosophila* wing. *Mechanisms of Development*, *144*, 23–32. https://doi.org/10.1016/j.mod.2016.10.003

Duell, B. L., Cripps, A. W., Schembri, M. A., & Ulett, G. C. (2011). Epithelial Cell Coculture Models for Studying Infectious Diseases: Benefits and Limitations. *Journal of Biomedicine and Biotechnology*, *2011*, 1–9. https://doi.org/10.1155/2011/852419

Enomoto, M., & Igaki, T. (2011). Deciphering tumor-suppressor signaling in flies: Genetic link between Scribble/Dlg/Lgl and the Hippo pathways. *Journal of Genetics and Genomics*, *38*(10), 461–470. https://doi.org/10.1016/j.jgg.2011.09.005

Fire, A., Albertson, D. G., Harrison, S. W., & Moerman, D. G. (1991). Production of antisense RNA leads to effective and specific inhibition of gene expression in *C. elegans* muscle. *Development*, *113*(2), 503–514. https://doi.org/10.1242/dev.113.2.503

Fire, A., Xu, S., Montgomery, M. W., Kostas, S. A., Driver, S. E., & Mello, C. C. (1998). Potent and specific genetic interference by double-stranded RNA in *Caenorhabditis elegans*. *Nature*, *391*(6669), 806–811. https://doi.org/10.1038/35888

Fischbach, L. (2022). Investigating the molecular mechanisms underlying intercellular regulation of apicobasal polarity in *Drosophila* wing imaginal disc. MSc thesis at Helsingin yliopisto (University of Helsinki). http://urn.fi/URN:NBN:fi:hulib-202207043149

Fortini, M. E., Skupski, M. P., Boguski, M. S., & Hariharan, I. K. (2000). A Survey of Human Disease Gene Counterparts in the *Drosophila* Genome. *Journal of Cell Biology*, *150*(2), F23–F30. https://doi.org/10.1083/jcb.150.2.f23

Friedman, A. J., & Perrimon, N. (2004). Genome-wide high-throughput screens in functional genomics. *Current Opinion in Genetics & Development*, *14*(5), 470–476. https://doi.org/10.1016/j.gde.2004.07.010

Gui, J., Huang, Y., Myllymäki, S., Mikkola, M., & Shimmi, O. (2021). Intercellular alignment of apical-basal polarity coordinates tissue homeostasis and growth. *BioRxiv*. https://doi.org/10.1101/2021.10.11.463906

Hales, K. H., Korey, C. A., Larracuente, A. M., & Roberts, D. D. (2015). Genetics on the Fly: A Primer on the *Drosophila* Model System. *Genetics*, *201*(3), 815–842. https://doi.org/10.1534/genetics.115.183392

Harris, T. J. C. (2012). Adherens Junction Assembly and Function in the *Drosophila* Embryo. *International Review of Cell and Molecular Biology*, 45–83. https://doi.org/10.1016/b978-0-12-394304-0.00007-5

Hatori, R., & Kornberg, T. B. (2020). Hedgehog produced by the *Drosophila* wing imaginal disc induces distinct responses in three target tissues. Development, 147(22). https://doi.org/10.1242/dev.195974

He, L., Binari, R., Huang, J., Falo-Sanjuan, J., & Perrimon, N. (2019). In vivo study of gene expression with an enhanced dual-color fluorescent transcriptional timer. *eLife*, *8*. https://doi.org/10.7554/elife.46181

Helft, L., Reddy, V., Chen, X., Koller, T., Federici, L., Fernández-Recio, J., Gupta, R., & Bent, A. F. (2011). LRR Conservation Mapping to Predict Functional Sites within Protein Leucine-Rich Repeat Domains. *PLOS ONE*, *6*(7), e21614. https://doi.org/10.1371/journal.pone.0021614

Higashi, T., & Miller, A. C. (2017). Tricellular junctions: how to build junctions at the TRICkiest points of epithelial cells. *Molecular Biology of the Cell*, *28*(15), 2023–2034. https://doi.org/10.1091/mbc.e16-10-0697

Holly, J. M. P., Zeng, L., & Perks, C. M. (2013). Epithelial cancers in the post-genomic era: should we reconsider our lifestyle? *Cancer and Metastasis Reviews*, *32*(3–4), 673–705. https://doi.org/10.1007/s10555-013-9445-5

Huang, Y., Gui, J., Myllymäki, S., Mikkola, M. L., & Shimmi, O. (2023). Coordination of tissue homeostasis and growth by the Scribble-α-Catenin-Septate junction complex. *IScience*, 106490. https://doi.org/10.1016/j.isci.2023.106490

Huang, Y., Gui, J., Myllymäki, S., Roy, K. K., Tõnissoo, T., Mikkola, M. L., & Shimmi, O. (2022). Scribble and α-Catenin cooperatively regulate epithelial homeostasis and growth. *Frontiers in Cell and Developmental Biology*, *10*. https://doi.org/10.3389/fcell.2022.912001

Inagaki, H. K., Jung, Y., Hoopfer, E. D., Wong, A. K. Y., Mishra, N., Lin, J., Tsien, R. Y., & Anderson, D. E. (2014). Optogenetic control of *Drosophila* using a red-shifted channelrhodopsin reveals experience-dependent influences on courtship. *Nature Methods*, *11*(3), 325–332. https://doi.org/10.1038/nmeth.2765

Jung, H., Fattet, L., Tsai, J. T. H., Kajimoto, T., Chang, Q., Newton, A. C., & Yang, J. (2019). Apical–basal polarity inhibits epithelial–mesenchymal transition and tumour metastasis by PAR-complex-mediated SNAI1 degradation. *Nature Cell Biology*, *21*(3), 359–371. https://doi.org/10.1038/s41556-019-0291-8

Kapil, S., Sharma, B. K., Patil, M., Elattar, S., Yuan, J., Hou, S. X., Kolhe, R., & Satyanarayana, A. (2017). The cell polarity protein Scrib functions as a tumor suppressor in liver cancer. *Oncotarget*, *8*(16), 26515–26531. https://doi.org/10.18632/oncotarget.15713

Lam, G., Beebe, K. L., & Thummel, C. S. (2022). A direct-drive GFP reporter for studies of tracheal development in *Drosophila*. *Fly*, *16*(1), 105–110. https://doi.org/10.1080/19336934.2022.2030191

Lessing, D., & Bonini, N. M. (2009). Maintaining the brain: insight into human neurodegeneration from *Drosophila melanogaster* mutants. *Nature Reviews Genetics*, *10*(6), 359–370. https://doi.org/10.1038/nrg2563

Letsou, A., & Bohmann, D. (2005). Small flies? Big discoveries: Nearly a century of *Drosophila* genetics and development. *Developmental Dynamics*, *232*(3), 526–528. https://doi.org/10.1002/dvdy.20307

Mese, G., Richard, G., & White, T. P. (2007). Gap Junctions: Basic Structure and Function. *Journal of Investigative Dermatology*, *127*(11), 2516–2524. https://doi.org/10.1038/sj.jid.5700770

Miller, D., Cook, K. H., & Hawley, R. S. (2019). The joy of balancers. *PLOS Genetics*, *15*(11), e1008421. https://doi.org/10.1371/journal.pgen.1008421

Mirzoyan, Z., Sollazzo, M., Allocca, M., Valenza, A., Grifoni, D., & Bellosta, P. (2019). *Drosophila melanogaster*: A Model Organism to Study Cancer. *Frontiers in Genetics*, *10*, 51. https://doi.org/10.3389/fgene.2019.00051

Moscat, J., & Diaz-Meco, M. T. (2000). The atypical protein kinase Cs. *EMBO Reports*, *1*(5), 399–403. https://doi.org/10.1093/embo-reports/kvd098

Müller, H. J. (2000). Genetic control of epithelial cell polarity: Lessons from *Drosophila*. *Developmental Dynamics*, *218*(1), 52–67. https://doi.org/10.1002/(sici)1097-0177(200005)218:1

Nainu, F., Salim, E., As'ad, M. F., Chandran, D., Dhama, K., Rabaan, A. A., & Emran, T. B. (2023). Fruit fly for anticancer drug discovery and repurposing. *Annals of Medicine and Surgery*, *85*(2), 337–342. https://doi.org/10.1097/ms9.0000000000000222

Neto-Silva, R. M., Wells, B. S., & Johnston, L. (2009). Mechanisms of Growth and Homeostasis in the *Drosophila* Wing. *Annual Review of Cell and Developmental Biology*, *25*(1), 197–220. https://doi.org/10.1146/annurev.cellbio.24.110707.175242

Nolan, M. E., Aranda, V., Lee, S., Lakshmi, B., Basu, S., Allred, D. C., & Muthuswamy, S. K. (2008). The Polarity Protein Par6 Induces Cell Proliferation and Is Overexpressed in Breast Cancer. *Cancer Research*, *68*(20), 8201–8209. https://doi.org/10.1158/0008-5472.can-07-6567

Ong, C. N., Yung, L. L., Cai, Y., Bay, B., & Baeg, G. H. (2015). *Drosophila melanogaster* as a model organism to study nanotoxicity. *Nanotoxicology*, *9*(3), 396–403. https://doi.org/10.3109/17435390.2014.940405

Ostalé, C. M., Ruiz-Gómez, A., Vega, P., Losada, M., Estella, C., & De Celis, J. F. (2018). *Drosophila* Imaginal Discs as a Playground for Genetic Analysis: Concepts, Techniques and Expectations for Biomedical Research. *InTech EBooks*. https://doi.org/10.5772/intechopen.72758

Osterwalder, T., Yoon, K. K., White, B., & Keshishian, H. (2001). A conditional tissue-specific transgene expression system using inducible GAL4. *Proceedings of the National Academy of Sciences of the United States of America*, *98*(22), 12596–12601. https://doi.org/10.1073/pnas.221303298

Rice, C., De, O., Alhadyian, H., Hall, S. A., & Ward, R. (2021). Expanding the Junction: New Insights into Non-Occluding Roles for Septate Junction Proteins during Development. *Journal of Developmental Biology*, *9*(1), 11. https://doi.org/10.3390/jdb9010011

Riga, A., Castiglioni, V. G., & Boxem, M. (2020). New insights into apical-basal polarization in epithelia. *Current Opinion in Cell Biology*, *62*, 1–8. https://doi.org/10.1016/j.ceb.2019.07.017

Roote, J. (2023). How to design a genetic mating scheme: a basic training package for *Drosophila* genetics. *Figshare*. https://doi.org/10.6084/m9.figshare.106631.v34
Roote, J., & Russell, S. (2012). Toward a complete *Drosophila* deficiency kit. *Genome Biology*, *13*(3). https://doi.org/10.1186/gb-2012-13-3-149

Rust, K., & Wodarz, A. (2021). Transcriptional Control of Apical-Basal Polarity Regulators. *International Journal of Molecular Sciences*, *22*(22), 12340. https://doi.org/10.3390/ijms222212340

Santoni, M., Kashyap, R., Camoin, L., & Borg, J. (2020). The Scribble family in cancer: twentieth anniversary. *Oncogene*, *39*(47), 7019–7033. https://doi.org/10.1038/s41388-020-01478-7

Sen, A., Nagy-Zsvér-Vadas, Z., & Krahn, M. P. (2012). *Drosophila* PATJ supports adherens junction stability by modulating Myosin light chain activity. *Journal of Cell Biology*, *199*(4), 685–698. https://doi.org/10.1083/jcb.201206064

Snigdha, K., Gangwani, K., Lapalikar, G. V., Singh, A., & Kango-Singh, M. (2019). Hippo Signaling in Cancer: Lessons From *Drosophila* Models. *Frontiers in Cell and Developmental Biology*, *7*. https://doi.org/10.3389/fcell.2019.00085

Stebbings, L., Todman, M. G., Phillips, R. B., Greer, C. W., Tam, J., Phelan, P., Jacobs, K., Bacon, J. P., & Davies, J. C. (2002). Gap junctions in *Drosophila*: developmental expression of the entire innexin gene family. *Mechanisms of Development*, *113*(2), 197–205. https://doi.org/10.1016/s0925-4773(02)00025-4

Su, W., Mruk, D. D., Wong, E. W., Lui, W., & Cheng, C. H. (2012). Polarity Protein Complex Scribble/Lgl/Dlg And Epithelial Cell Barriers. *Advances in Experimental Medicine and Biology*, 149–170. https://doi.org/10.1007/978-1-4614-4711-5_7

Sun, F. F., Johnson, J. E., Zeidler, M. P., & Bateman, J. R. (2012). Simplified Insertion of Transgenes Onto Balancer Chromosomes via Recombinase-Mediated Cassette Exchange. *G3: Genes, Genomes, Genetics*, *2*(5), 551–553. https://doi.org/10.1534/g3.112.002097

Sun, Y., Yolitz, J., Wang, C. C. L., Spangler, E. L., Zhan, M., & Zou, S. (2013). Aging Studies in *Drosophila Melanogaster*. *Humana Press eBooks*, 77–93. https://doi.org/10.1007/978-1-62703-556-9_7

Tadeu, A. M. B., & Horsley, V. (2014). Epithelial Stem Cells in Adult Skin. *Elsevier EBooks*, 109–131. https://doi.org/10.1016/b978-0-12-416022-4.00004-4

Tripathi, B. K., & Irvine, K. D. (2022). The wing imaginal disc. *Genetics*, *220*(4). https://doi.org/10.1093/genetics/iyac020

Van De Leemput, J., & Han, Z. (2021). *Drosophila*, a powerful model to study virus-host interactions and pathogenicity in the fight against SARS-CoV-2. *Cell & Bioscience*, *11*(1). https://doi.org/10.1186/s13578-021-00621-5

Venken, K., Simpson, J. A., & Bellen, H. J. (2011). Genetic Manipulation of Genes and Cells in the Nervous System of the Fruit Fly. *Neuron*, *72*(2), 202–230. https://doi.org/10.1016/j.neuron.2011.09.021

Verghese, S., Waghmare, I., Kwon, H. J., Hanes, K., & Kango-Singh, M. (2012). Scribble Acts in the *Drosophila* Fat-Hippo Pathway to Regulate Warts Activity. *PLOS ONE*, *7*(11), e47173. https://doi.org/10.1371/journal.pone.0047173

Wangler, M. F., & Bellen, H. J. (2017). In Vivo Animal Modeling. *Basic Science Methods for Clinical Researchers*, 211–234. https://doi.org/10.1016/b978-0-12-803077-6.00012-6

Wright, A. M., Fox, A. N., Johnson, K. M., & Zinn, K. (2010). Systematic Screening of *Drosophila* Deficiency Mutations for Embryonic Phenotypes and Orphan Receptor Ligands. *PLOS ONE*, *5*(8), e12288. https://doi.org/10.1371/journal.pone.0012288

Yu, J., & Pan, D. (2018). Validating upstream regulators of Yorkie activity in Hippo signaling through *scalloped*-based genetic epistasis. *Development*, *145*(4). https://doi.org/10.1242/dev.157545

Zeitler, J., Hsu, C., Dionne, H., & Bilder, D. (2004). Domains controlling cell polarity and proliferation in the *Drosophila* tumor suppressor Scribble. *Journal of Cell Biology*, *167*(6), 1137–1146. https://doi.org/10.1083/jcb.200407158

Zeng, X., Chauhan, C., & Hou, S. X. (2013). Stem Cells in the *Drosophila* Digestive System. *Advances in Experimental Medicine and Biology*, 63–78. https://doi.org/10.1007/978-94-007-6621-1_5

NON-EXCLUSIVE LICENCE TO REPRODUCE THESIS AND MAKE THESIS PUBLIC

I, Gleb Zenjov

1. herewith grant the University of Tartu a free permit (non-exclusive licence) to reproduce, for the purpose of preservation, including for adding to the DSpace digital archives until the expiry of the term of copyright,

"Screening of genes vital for the epithelial homeostasis with Scribble in Drosophila imaginal wing disc morphogenesis",
supervised by Osamu Shimmi and Hanna Antson.

2. I grant the University of Tartu a permit to make the work specified in p. 1 available to the public via the web environment of the University of Tartu, including via the DSpace digital archives, under the Creative Commons licence CC BY NC ND 3.0, which allows, by giving appropriate credit to the author, to reproduce, distribute the work and communicate it to the public, and prohibits the creation of derivative works and any commercial use of the work until the expiry of the term of copyright.

3. I am aware of the fact that the author retains the rights specified in p. 1 and 2.

4. I certify that granting the non-exclusive licence does not infringe other persons' intellectual property rights or rights arising from the personal data protection legislation.

Gleb Zenjov
24/05/2023